الجمهورية الجزائرية الديمقراطية الشعبية

PEOPLE'S DEMOCRATIC REPUBLIC OF ALGERIA

وزارة التعليم العالي و البحث العلمي

Ministry of Higher Education and Scientific Research

جامعة أبي بكر بلقايد – تلمسان –

University of Aboubakr Belkaid – Tlemcen –

Faculty of TECHNOLOGY

MEMOIR

Presented for the attainment of **MASTER's Degree**

In: Electronic

Specialization: INSTRUMENTATION

By: HACHIM Mohammed

Subject

Modeling of amplifier circuits using transfer functions and simulations in Proteus 8 Professional

Publicly defended in June 2025, before the jury composed of:

Mr Benyarou Mourad	SLCA	University of Tlemcen	President
Mme Benbekhti Fatiha	SLCB	University of Tlemcen	Examiner
Mr Benahmed Nasreddine	Professor	University of Tlemcen	Supervisor
Mme Benabdallah Nadia	Professor	ESSA-Tlemcen	Co-Supervisor

Academic Year: 2024 / 2025

Acknowledgements

I would like to express my deep gratitude to all the members of the jury who kindly honored this defense with their presence and expertise.

I particularly thank Mr. Benyarou Mourad, President of the jury, for agreeing to evaluate my work and for his constructive remarks.

I also wish to thank Mrs. Benbekhti Fatiha for the time she devoted to reading this thesis and for her enriching observations.

My gratitude also goes to Mr. Benahmed Nasreddine, my supervisor, for his valuable advice, attentive follow-up, availability, and support throughout this work. His guidance was of great importance in the realization of this thesis.

I also thank Mrs. Benabdallah Nadia, co-supervisor, for her scientific support and her pertinent suggestions which allowed for a deeper analysis of the subject treated.

Finally, I wish to extend my thanks to all the people who, near or far, contributed to the success of this work.

ملخص المشروع

يندرج هذا المشروع لنهاية الدراسة ضمن مجال الإلكترونيات التماثلية، ويهدف أساسًا إلى تحليل ونمذجة ومحاكاة دوائر المضخمات المعتمدة على الترانزستورات الثنائية القطبية (BJT) والمضخمات العملياتية (ampli-op) باستخدام بيئة المحاكاة (Proteus 8 Professional) .

وقد تمحور العمل حول أربعة محاور رئيسية:

الدراسة النظرية و النمذجة في المجال الترددي: تم تقديم حالة فنية مفصلة حول الخصائص الكهربائية للترانزستورات الثنائية القطبية (مثل معامل التكبير في التيار، وتردد الانتقال، والمقاومات الطفيلية) والمضخمات العملياتية (مثل معامل التكبير في الدائرة المفتوحة، وعرض الحزمة، والاستجابة الترددية). كما تم صياغة دوال الانتقال لهذه المكونات في نطاق لابلاس.

التحقق من صحة طريقة بن أحمد: تم تطبيق نهج تحليلي صارم لحساب مقاومات الانحياز وتحديد دالة الانتقال لمضخم يعمل في وضع المجمع المشترك مع باعث مفصول. وقد تم التحقق من صحة النتائج النظرية من خلال محاكاة زمنية وترددية باستخدام (Proteus) .

تطوير نموذج (SPICE) افتراضي: تم تصميم نموذج مخصص لترانزستور يتميز بتردد انتقال مرتفع ($f_T = 1$ GHz) وتم إدماجه في مكتبة (Proteus) ، مما أتاح إمكانية استكشاف أداء المضخمات في الترددات العالية جدًا.

محاكاة وتحليل النتائج: تمت مقارنة الاستجابات الترددية والديناميكية للدارات المحاكاة مع النماذج التحليلية. وقد ساعدت الفروقات الملحوظة في فهم تأثير العناصر الطفيلية والقيود الفيزيائية على الأداء الفعلي للمضخمات.

ساهم هذا المشروع في تعزيز المهارات في تصميم الدارات التماثلية، النمذجة الرياضية، والمحاكاة العددية، وفتح آفاقًا مستقبلية نحو تصميم دارات متكاملة عالية التردد وتحسين أدائها في الأنظمة الإلكترونية المعقدة.

Résumé du Projet

Ce projet de fin d'études s'inscrit dans le domaine de l'électronique analogique, avec pour objectif principal l'analyse, la modélisation et la simulation de circuits amplificateurs à transistors bipolaires (BJT) et amplificateurs opérationnels (ampli-op) à l'aide de l'environnement Proteus 8 Professional.

Le travail s'est articulé autour de quatre axes principaux :

Étude théorique et modélisation fréquentielle : Un état de l'art détaillé a été établi sur les caractéristiques électriques des transistors bipolaires (gain en courant, fréquence de transition, résistances parasites) et des amplis-op (gain en boucle ouverte, bande passante, réponse en fréquence). Les fonctions de transfert de ces dispositifs ont été formulées dans le domaine de Laplace.

Validation de la méthode de Benahmed : Une approche analytique rigoureuse a été appliquée pour dimensionner les résistances de polarisation et déterminer la fonction de transfert d'un amplificateur à transistor en configuration émetteur commun avec émetteur découplé. Les résultats ont été validés par des simulations temporelles et fréquentielles sous Proteus.

Développement d'un modèle SPICE fictif : Un modèle de transistor personnalisé avec une fréquence de transition élevée (f_T = 1 GHz) a été conçu et intégré dans la bibliothèque de Proteus, permettant d'explorer les performances d'amplificateurs en très haute fréquence.

Simulation et interprétation des résultats : Les réponses fréquentielles et dynamiques des circuits simulés ont été comparées aux modèles analytiques. Les écarts observés ont permis de mieux comprendre l'influence des effets parasites et des limitations physiques sur la performance réelle des circuits.

Ce projet a permis de consolider les compétences en conception de circuits analogiques, modélisation mathématique, simulation numérique, tout en ouvrant des perspectives vers la conception de circuits intégrés à haute fréquence et l'optimisation des performances dans des systèmes électroniques complexes.

Project Summary

This final-year project falls within the field of analog electronics, with the primary objective of analyzing, modeling, and simulating amplifier circuits based on bipolar junction transistors (BJTs) and operational amplifiers (op-amps) using the Proteus 8 Professional simulation environment.

The work was structured around four main pillars:

Theoretical Study and Frequency-Domain Modeling: A detailed state of the art was established covering the electrical characteristics of BJTs (current gain, transition frequency, parasitic resistances) and op-amps (open-loop gain, bandwidth, frequency response). The transfer functions of these devices were formulated in the Laplace domain.

Validation of the Benahmed Method: A rigorous analytical approach was applied to determine the biasing resistances and derive the transfer function of a common-emitter BJT amplifier with a decoupled emitter. The theoretical results were validated through both time-domain and frequency-domain simulations in Proteus.

Development of a Fictitious SPICE Model: A custom transistor model with a high transition frequency (f_T = 1 GHz) was designed and integrated into the Proteus library, allowing the simulation of amplifiers operating at very high frequencies.

Simulation and Interpretation of Results: The simulated frequency and time responses of the circuits were compared with their analytical models. The discrepancies observed provided valuable insights into the impact of parasitic effects and physical limitations on real-world amplifier performance.

This project strengthened skills in analog circuit design, mathematical modeling, and numerical simulation, while also opening pathways toward the design of high-frequency integrated circuits and performance optimization in complex electronic systems.

Table of contents

General Introduction

Analog electronics constitute a fundamental field in the design of embedded systems, telecommunications, instrumentation, and signal processing. At the core of this discipline, amplifier circuits play a strategic role in ensuring signal conditioning, amplification, and fidelity, whether they originate from sensors or other functional blocks. With the increasing complexity of electronic systems and the heightened requirements for performance and reliability, precise modeling and rigorous simulation of amplification circuits have become indispensable, particularly in high-frequency applications.

In this context, the present thesis focuses on studying and modeling two fundamental types of amplifiers: bipolar junction transistor (BJT) amplifiers and operational amplifiers (op-amps). The work relies on advanced simulation tools, including Proteus 8 Professional, Excel, Origin, and SPICE models, to effectively bridge theoretical models with the real behavior of circuits.

The thesis is structured around four complementary chapters, each addressing a fundamental aspect of this topic :

Chapter 1 is dedicated to the state of the art. It provides a detailed overview of the physical principles and electrical characteristics of bipolar transistors and operational amplifiers. Essential concepts such as current gain (β), transition frequency (f_T), parasitic internal resistances, and the frequency dynamics of op-amps like the μA741 are introduced. This chapter establishes the theoretical foundation necessary to understand the phenomena under study.

Chapter 2 focuses on the experimental validation of a rigorous analytical model based on the Benahmed method. This method enables the direct calculation of bias resistances and the analytical formulation of the transfer function of a common-emitter BJT amplifier. Simulations in Proteus verify the agreement between theoretical results and the actual circuit behavior, both in the time domain and frequency domain.

Chapter 3 is devoted to the modeling of op-amp amplifiers, particularly in inverting and non-inverting configurations. By analyzing the actual frequency response of an op-amp, this chapter highlights the limitations due to finite gain and reduced bandwidth. It then develops a precise formulation of the transfer function, considering non-ideal characteristics, and validates these results through numerical simulations.

Chapter 4 presents a forward-looking approach, developing a hypothetical SPICE model of an ultra-high-frequency bipolar transistor (f_T = 1 GHz). Designed to exceed the physical limits of standard components, this model is integrated into the Proteus library and subsequently used to simulate high-frequency amplifiers, paving the way for advanced designs intended for radiofrequency applications and high-speed communications.

Each section contributes to building a coherent bridge between theory and practice by implementing reliable analytical models, precise simulations, and critical analysis of results. The overall project thus demonstrates the ability to design, evaluate, and optimize complex analog circuits in response to the increasing demands of modern electronics.

Chapter 1: State of the Art on Bipolar Transistor Amplifiers and Operational Amplifier-Based Amplifier

1.1 Introduction

Amplifiers play a fundamental role in electronics by amplifying weak signals while preserving their characteristics. Among the most common types are bipolar transistor amplifiers and operational amplifiers (op-amps) [1].

In this project, we focus on modeling these amplifiers using Proteus 8 Professional, an advanced simulation tool [2]. We will examine the essential characteristics of their active components, including:

- **For a bipolar transistor:** current gain, input resistance, output resistance, and transition frequency (f_T), which depends on the specific transistor used (e.g., for a BC550, $f_T \approx 227\ MHz$) [3].
- **For an op-amp:** open-loop gain (A_{vo}), bandwidth limited by its high frequency (f_{h}), and transition frequency (f_T). For example, the µA741 op-amp, has a transition frequency of approximately $f_T \approx 1\ MHz$ [4].

The objectives of this project are to:

- Model these amplifiers in Proteus by extracting their transfer functions (p).
- Simulate their time-domain and frequency-domain responses.
- Export the frequency responses from Proteus to Excel and then to Origin 50 for more precise plotting and integration into the PFE report in DOC format [5].
- Develop a fictional SPICE model of a transistor with a high transition frequency of 1 GHz and integrate it into Proteus's library for future use [6].

This work will enhance our understanding of amplifier frequency behavior and help optimize designs for specific high-performance applications.

1.2 Bipolar Junction Transistor (BJT) and its characteristics

The **Bipolar Junction Transistor (BJT)** is a key semiconductor component used in analog and digital circuits [7]. It consists of three regions: emitter, base, and collector, and operates by controlling a large collector current (I_C) with a small base current (I_B).

BJTs can be used in various configurations, such as: Common Emitter (CE), Common Base (BC) and the Common Collector (CC), each has unique characteristics suited for different amplification and switching applications.

1.2.1 Key Electrical Characteristics of a BJT

- **Current Gain ($\boldsymbol{\beta}$)**

The current gain (β) is defined as the ratio of collector current to base current:

$$\beta = \frac{I_C}{I_B}$$

This parameter depends on the transistor, the bias current, and the temperature. For the BC550, β ranges from 110 to 800 depending on collector current.

- **Base-Emitter Threshold Voltage (V_{BE})**

A bipolar transistor requires a minimum voltage to start conducting. In forward bias mode, this voltage is approximately:

$V_{BE} \approx 0.7V$ for silicon transistors.

$V_{BE} \approx 0.3V$ for germanium transistors.

- **Transition Frequency (f_T)**

The transition frequency (f_T) of a bipolar junction transistor (BJT) is a key parameter that defines the frequency at which the transistor's current gain becomes equal to 1 in high-frequency operation.

In other words, it is the frequency at which the open-loop current gain (β) drops to unity. This parameter is crucial for high-frequency applications as it determines the transistor's dynamic performance. It is given by:

$$f_T = \frac{I_C}{2\pi \times U_T \times C_e}$$

Where:

I_C is the collector current (in A).

U_T is the thermal voltage (26 mV at ambient temperature).

C_e is the emitter capacitance (in F).

Application on the BC550 transistor:

For a BC550 transistor with the following values: I_C = 1.6mA, C_e = 43pF and U_T = 26mV, the transition frequency is calculated as follows:

$$f_T = \frac{1.6 \times 10^{-3}}{2\pi \times 26 \times 10^{-3} \times 43 \times 10^{-12}}$$

$$f_T \approx 227.8\, MHz$$

This result means that the BC550 transistor is usable up to approximately 200 MHz before its current gain β becomes insufficient [8].

- **Parasitic Resistances**

A bipolar transistor has internal resistances that influence its frequency performance. These include:

r_{be} $(or\ h_{11})$: base-emitter resistance,

r_{ce} $(or\ h_{22}^{-1})$: collector-emitter resistance,

r_{bb}: internal base resistance.

These resistances affect the frequency response and stability of the transistor in amplifier circuits

1.2.2 Dependency of transistor characteristics

- **Collector current I_C**

- The transition frequency f_T increases with the collector current I_C up to a certain limit.

- Beyond this limit, space-charge effects reduce f_T.

- **Temperature**

When the temperature increases, the thermal voltage U_T rises, and the emitter capacitance C_e may change, which reduces the transition frequency f_T.

- **Transistor Architecture**

Advanced technologies, such as heterojunction bipolar transistors (HBTs), allow for very high transition frequencies (exceeding several hundred GHz).

1.2.3 Impact on Amplifiers

The electrical characteristics of a BJT (Bipolar Junction Transistor) play a key role in amplifier design:

- A high transition frequency allows for a wide bandwidth, which is crucial for high-frequency applications.
- A low base-emitter resistance r_{be} $(ou\ h_{11})$ improves the transistor's frequency response.
- The choice of bias current I_C optimizes frequency performance.

These parameters must be carefully considered when designing amplifiers using bipolar transistors to ensure optimal performance.

1.3 Common Emitter Bipolar Amplifier

A bipolar transistor amplifier can be implemented in a common-emitter configuration, where it provides a significant voltage gain.

1.3.1 Transfer Function

In this configuration, the transfer function follows a low-pass model.

$$A(p) = -\frac{|A_v|}{1 + \frac{p}{2\pi f_h}}$$

Where:

The negative sign (-) indicates that the input and output signals are phase-opposed.

p is the Laplace variable.

$|A_v|$ represents the low-frequency gain.

f_h is the upper frequency limit of the bandwidth.

The gain-bandwidth product of the amplifier is defined as (see later) : $|A_v| \times f_h = f_T$ [9].

The higher the transition frequency f_T, the wider the bandwidth of an amplifier with a fixed voltage gain $|A_v|$.

The previous expression is equivalent to:

$$A(p) = -\frac{|A_v|}{1 + \frac{|A_v|\, p}{2\pi f_T}}$$

In an ideal case, where parasitic effects such as Miller effect and parasitic capacitances are negligible, the transition frequency of a single-stage common-emitter amplifier is almost equal to the transition frequency of the transistor used. This means that the relation: $|A_v| \times f_h = f_T$ applies directly, where f_T corresponds to the frequency at which the current gain of the transistor becomes unity. Thus, under these ideal conditions, the amplifier's bandwidth does not experience significant reduction compared to the intrinsic characteristics of the transistor, and the high cutoff frequency f_h follows directly from the gain-bandwidth product relation.

1.4 Operational Amplifiers

Operational amplifiers, often abbreviated as op-amps, are fundamental electronic components widely used in analog electronics. They serve various functions, including amplification, filtering, summation, differentiation, integration, and much more [10].

An ideal operational amplifier has the following characteristics:

- Very high open-loop gain A_{v0} (theoretically infinite),
- Very high input impedance (ideally infinite),
- Very low output impedance (ideally zero),
- Wide bandwidth, allowing amplification of signals over a broad frequency range,
- High common-mode rejection ratio (CMRR or TRMC) (>80 dB), which helps eliminate unwanted signals that appear identically on both inputs.

However, in practice, real operational amplifiers have limitations, including a finite bandwidth often quite low (sometimes just a few Hz) and an open-loop gain that varies with frequency.

1.4.1 Frequency Response of an Operational Amplifier: The Case of the µA741

One of the essential parameters of operational amplifiers is their frequency response. Figure 1 illustrates this response for the µA741 op-amp, a widely used model in standard applications.

➢ **Analysis of the Figure**

This figure represents the curve of the open-loop differential gain as a function of frequency:

- **Open-Loop Gain A_{v0}**

- At low frequencies, the µA741 exhibits a maximum gain of approximately 106 dB (which corresponds to 200,000 in linear terms).

- This gain gradually decreases as the frequency increases.

- **Bandwidth and cutoff frequency (-3 dB)**

- The frequency at which the gain drops by 3 dB is approximately 5 Hz.

- Beyond this frequency, the open-loop differential gain A_{v0} decreases at a rate of -20 dB per decade (a slope of -1).

- **Transition Frequency (f_T)**

- The gain reaches 0 dB (a factor of 1 in linear scale) at a frequency of 1 MHz.

- This frequency corresponds to the gain-bandwidth product $A_{v0} \times f_h = f_T$, which remains constant.

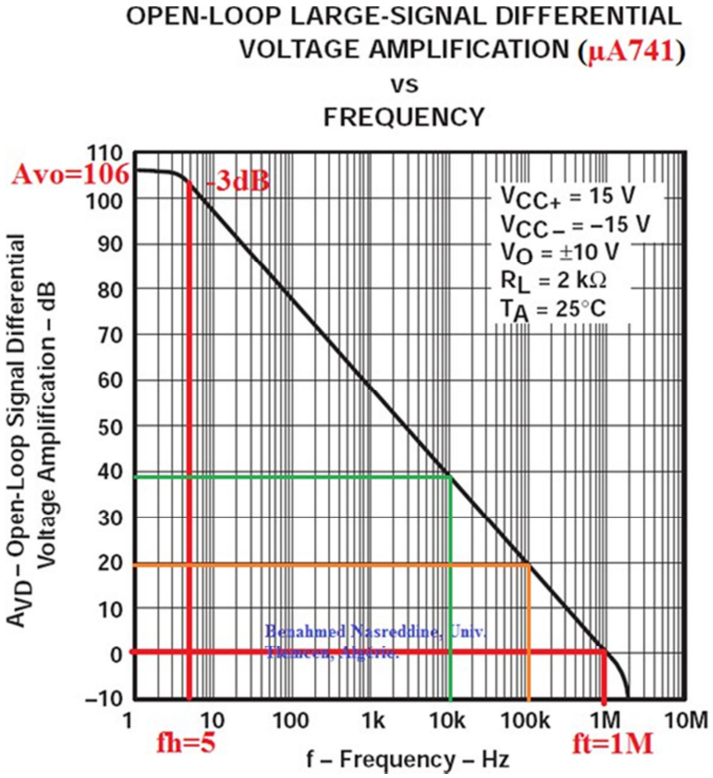

Figure 1: Open-Loop frequency response of a real operational amplifier: case of the µA741

➢ **Practical Consequences**

- In open-loop configuration, the operational amplifier can only effectively process very low-frequency signals (< 5 Hz).
- In closed-loop configuration, thanks to negative feedback, it is possible to extend the bandwidth by reducing the gain.

This behavior limits the use of the μA741 in high-frequency applications unless appropriate compensation is applied.

1.4.2 Transfer Function of an Operational Amplifier

The study of the frequency response of an operational amplifier naturally leads to the analysis of its transfer function.

In open-loop configuration, the frequency response of the gain of a real operational amplifier follows the dynamics of a first-order low-pass filter.

The mathematical expression for the open-loop differential gain transfer function is given by :

$$A(p) = \frac{A_{vo}}{1 + \frac{p}{2\pi f_h}} = \frac{2\pi A_{vo} f_h}{p + 2\pi f_h}$$

A_{v0} is the open-loop gain at very low frequencies (DC) (~200,000 or 106 dB for the μA741).

p represents the Laplace variable.

f_h is the cutoff frequency at -3 dB (with $f_h \approx 5Hz$ for the μA741).

- **Physical Interpretation**

At very low frequencies $f \ll f_h \rightarrow$ the gain remains practically constant and equal to A_{VO}.

At the cutoff frequency $f_h \rightarrow$ the gain drops by 3 dB (which corresponds to a division by $\sqrt{2}$ in amplitude).

At high frequencies $f \gg f_h \rightarrow$ the gain decreases proportionally to frequency with a slope of -20 dB per decade.

At the transition frequency $f_T = A_{vo} \times f_h$ (~1 MHz for the μA741) → the gain reaches 1 (0 dB), marking the limit of effective amplification.

This behavior can be represented in an asymptotic Bode plot (Figure 2), where a linear decrease in gain (in dB) beyond f_h is observed in the frequency domain.

For the μA741, the relevant values are (Figure 2):

Open-loop gain: $A_{vo} = 106\ dB = 2 \times 10^5$.

Cutoff frequency (-3 dB) : $f_h = 5Hz \rightarrow \omega_h = 2\pi f_h = 31.4\ rd/s$.

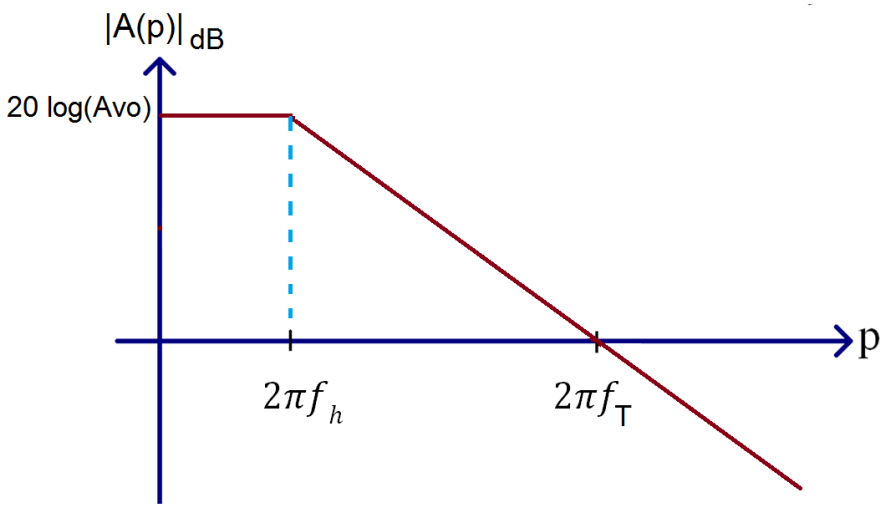

Figure 2: Asymptotic Bode plot of the open-loop voltage gain of a real operational amplifier

Therefore, the transfer function of the µA741 is given by:

$$A(p) = \frac{A_{vo}}{1 + \frac{p}{2\pi f_h}} = \frac{A_{vo}}{1 + \frac{p}{\omega_h}}$$

By substituting the numerical values:

$$A(p)|_{\mu A741} = \frac{2 \times 10^5}{1 + \frac{p}{31.4}} \leftrightarrow A(p)|_{\mu A741} = \frac{2 \times 10^5}{1 + 318.47 \times 10^{-4}\, p}$$

It is important to note that the transition frequency of an operational amplifier is identical to that of a non-inverting amplifier. However, in an inverting configuration, the transition frequency is slightly lower than that of open-loop or non-inverting configurations, due to the effects of negative feedback and associated impedances

1.5 Gain-Bandwidth and Frequency Limitations

The relationship between gain and bandwidth in an amplifier follows the gain-bandwidth product invariance:

$A_v \times f_h = constante$

This means that the higher the closed-loop gain, the narrower the bandwidth. This constraint often requires a trade-off between gain and bandwidth, especially in high-frequency applications. Thus, to design an amplifier while maintaining a sufficient gain, it is necessary to optimize both the components and the circuit structure.

1.6 Design and Simulation of Virtual Amplifiers in Proteus

1.6.1 Objective of the Modeling

One of the objectives of this project is to design and simulate a fictitious transistor amplifier in Proteus 8.12, capable of operating at high frequencies, beyond the limitations of a real component.

To achieve this, we will create an adaptable SPICE model for a customized bipolar transistor with a transition frequency of 1 GHz.

This model will then be integrated into the Proteus 8.12 library, allowing users to perform high-frequency simulations with enhanced performance.

1.6.2 Implementation Steps

The design and validation of the fictitious amplifier will follow several steps:

- Defining the electrical and frequency parameters of the fictitious transistor based on the SPICE model.
- Implementing the model in Proteus, incorporating these characteristics into a customizable component.
- Validating the model through time-domain and frequency-domain simulations to verify its high-frequency performance.
- Integrating the model into the Proteus library, enabling reuse in other designs and simulations.

This approach will allow us to explore the behavior of amplifiers at very high frequencies, without being restricted by the physical limitations of existing components.

1.7 Conclusion

This first chapter has established a rigorous state of the art on bipolar transistor amplifiers and operational amplifiers, highlighting their main electrical and frequency characteristics as well as their intrinsic limitations.

First, we studied bipolar transistors, detailing the key parameters influencing their amplification performance, including current gain (β), base-emitter voltage (V_{BE}), and transition frequency (f_T).

It was shown that, under ideal conditions, the transition frequency of a single-stage common emitter amplifier can be approximated to that of the transistor used. However, capacitive and parasitic effects can significantly restrict the actual bandwidth of the amplifier.

Next, the study of operational amplifiers allowed us to introduce their frequency response and examine the transfer function of real amplifiers, taking the µA741 op-amp as a reference. We demonstrated that this amplifier follows a first-order low-pass behavior, with a very low cutoff frequency ($f_h \approx 5\ Hz$) and a limited transition frequency of 1 MHz. We also highlighted the impact of the gain-bandwidth product, which requires a reduction in bandwidth when the closed-loop gain is increased.

Finally, in the context of transistor amplifiers, we introduced our innovative approach aimed at overcoming these limitations through the development of a high-frequency fictitious amplifier model in Proteus. This model is based on the integration of a fictitious bipolar transistor characterized by a high transition frequency ($f_T = 1\ GHz$).

Integrating this model into the Proteus library will be a major asset for the simulation and analysis of high-frequency bipolar transistor circuits, paving the way for advanced designs and better control of electronic systems.

The following chapters will focus on the methodology for extracting transfer functions, as well as the techniques for simulation and experimental validation of the developed models.

Bibliographic References

[1] P. Horowitz & W. Hill, The Art of Electronics, 3rd ed., Cambridge University Press, 2015.

[2] Official Documentation of Labcenter Electronics, Proteus Design Suite – Simulation and PCB Design Software, available at: www.labcenter.com.

[3] A. Sedra & K. Smith, Microelectronic Circuits, 7th ed., Oxford University Press, 2014.

[4] Texas Instruments, Operational Amplifier μA741 Datasheet, available at: www.ti.com.

[5] B. Razavi, Design of Analog CMOS Integrated Circuits, 2nd ed., McGraw-Hill, 2016.

[6] R. C. Jaeger & T. N. Blalock, Microelectronic Circuit Design, 5th ed., McGraw-Hill, 2015.

[7] P. Gray, P. Hurst, S. Lewis & R. Meyer, Analysis and Design of Analog Integrated Circuits, 5th ed., Wiley, 2009.

[8] J. Millman & A. Grabel, Microelectronics, 2nd ed., McGraw-Hill, 1987.

[9] R. Boylestad & L. Nashelsky, Electronic Devices and Circuit Theory, 11th ed., Pearson, 2012.

[10] National Semiconductor, AN-31: Op Amp Circuit Collection, 2000.

Chapter 2: Validation of Benahmed's Method for Determining the Transfer Function and Biasing Resistors of a Transistor Amplifier in Proteus

2.1 Introduction

The analysis and modeling of common-emitter bipolar amplifiers are essential for the design and optimization of analog circuits. To improve model accuracy and facilitate their integration into simulations, it is crucial to establish an analytical transfer function that accurately reflects the circuit's real behavior.

In this context, the Benahmed method offers a rigorous approach to determining not only the expression of the transfer function of a decoupled-emitter bipolar amplifier but also the optimal values of biasing resistances [1]. This method is based on a thorough analysis of bias equations and the frequency characteristics of the transistor to develop a complete model of gain as a function of frequency.

The objective of this chapter is to experimentally validate this method by comparing analytically computed results with simulations performed in Proteus. To achieve this, we follow a multi-step approach:

- Determining the biasing resistance values using the Benahmed method to ensure a stable operating point for the transistor.
- Theoretical establishment of the amplifier's transfer function using the same method.
- Frequency analysis in Proteus to compare the real circuit response with the theoretical transfer function.
- Time-domain analysis to verify whether replacing the amplifier with its transfer function yields an accurate dynamic response.

This study aims to demonstrate that the Benahmed method enables precise bias resistance design and the development of a reliable transfer function capable of replacing the amplifier in a simulation, thereby facilitating the optimization and analysis of electronic circuits.

2.2 Presentation of the Benahmed Method and Its Application to Common-Emitter Amplifiers with Decoupled Emitters

The Benahmed method is a rigorous and systematic approach used for the design of bipolar junction transistor (BJT) common-emitter (CE) amplifiers with decoupled emitters. This method allows for the direct determination of optimal component values based on design specifications, ensuring a stable operating point, precise voltage gain, and good frequency response [2, 3].

In a CE amplifier with a decoupled emitter, a bypass capacitor C_E is placed in parallel with the emitter resistance R_E. This capacitor effectively short-circuits R_E for AC signals, significantly increasing voltage gain by eliminating the negative feedback effect.

The main advantage of the Benahmed method lies in its precision and efficiency: it eliminates approximations and trial-and-error approaches by providing analytical formulas for sizing the circuit resistances according to transistor parameters and the required specifications.

2.2.1 Objectives and Advantages of the Benahmed Method

The objective of this method is to design a common-emitter amplifier with a decoupled emitter, ensuring (Figure 1):

• A precise voltage gain defined by:

$$A_v = -\frac{\beta\, R_C}{h_{11}}$$

• Stable transistor biasing to prevent signal distortion.

• Good frequency response, taking into account the transistor's internal capacitance.

• Fast and reproducible design, avoiding experimental trial-and-error.

This approach is particularly well-suited for circuits requiring high amplification and wide bandwidth, such as audio amplifiers, radio-frequency systems, and communication devices.

2.2.2 Steps of the Benahmed Method

The method is based on precise analytical calculations that allow for the determination of all circuit resistances from the transistor parameters and the desired specifications.

- **Calculation of the collector resistance $\mathbf{R_C}$**

$$A_v = -\frac{\beta\ R_C}{h_{11}} = -\frac{\beta\ R_C}{\frac{U_T}{I_{BQ}}} = -\frac{\beta\ I_{BQ}\ R_C}{U_T} = -\frac{I_{CQ}\ R_C}{U_T} = -\frac{R_C\ I_{CQ}}{U_T}$$

$$\rightarrow R_C = \frac{U_T\ \times\ (-A_v)}{I_{CQ}}$$

where U_T represents the thermal voltage (≈26 mV), A_v the voltage gain, and I_{CQ} the transistor bias current.

- **Calculation of the emitter voltage V_{EM}**

$$V_{EM} + V_{CEQ} + R_C\ I_{CQ} = V_{cc}$$

$$\rightarrow V_{EM} = \frac{V_{cc}}{2} - R_C\ I_{CQ}$$

$$\rightarrow V_{EM} = \frac{V_{cc}}{2} + A_v\ U_T$$

This equation allows for a centered operating point, ensuring good signal dynamics.

- **Calculation of the emitter voltage $\mathbf{R_E}$**

$$R_E = \frac{V_{EM}}{I_{CQ}}$$

$$R_E = \frac{\frac{V_{cc}}{2} + A_v\ U_T}{I_{CQ}}$$

This resistance stabilizes the transistor's current.

- **Calculation of the base voltage V_{BM}**

$$V_{BM} = V_{EM} + V_{BEQ}$$

where $V_{BEQ} = 0.7V$ is the base-emitter voltage of the transistor.

- **Bias current (I_p)**

$$I_p = 10 \times I_{BQ} = 10 \times \frac{I_{CQ}}{\beta}$$

- **Calculation of the biasing resistances R_{B1} and R_{B2}**

$$R_{B2} = \frac{V_{BM}}{I_p} = \frac{\beta(V_{EM} + V_{BEQ})}{10 \times I_{CQ}} = \frac{\beta\left(\frac{V_{cc}}{2} + A_v\, U_T + V_{BEQ}\right)}{10 \times I_{CQ}}$$

$$R_{B2} = \frac{\beta\left(\frac{V_{cc}}{2} + A_v\, U_T + V_{BEQ}\right)}{10 \times I_{CQ}}$$

$$R_{B1} = \frac{V_{cc} - V_{BM}}{11 \times I_{BQ}} = \frac{\beta(V_{cc} - V_{EM} - V_{BEQ})}{11 \times I_{CQ}}$$

$$R_{B1} = \frac{\beta\left(\frac{V_{cc}}{2} - A_v\, U_T - V_{BEQ}\right)}{11 \times I_{CQ}}$$

These expressions ensure stable thermal biasing, minimizing variations due to temperature changes.

2.2.3 Conclusion

The Benahmed method is a powerful tool for designing common-emitter amplifiers with a decoupled emitter. It ensures:

• Precise and optimized gain for the desired performance.

• Improved thermal and frequency stability.

• Reliable analytical design, eliminating trial-and-error approaches.

This method is particularly useful in advanced electronic applications requiring high amplification and wide bandwidth, such as RF circuits, audio amplifiers, and signal transmission systems.

2.3 Application of the Method

To apply the Benahmed method to the bipolar junction transistor (BJT) common-emitter amplifier with a decoupled emitter shown in Figure 1, we consider the following design specifications:

• Transistor: BC550

• Supply voltage: $V_{cc} = 12V$

• Current gain: $\beta = 132.5$

• Bias current: $I_{CQ} = 1.6mA$

• Voltage gain: $A_v = -100$

• Thermal voltage: $U_T = 26mV$

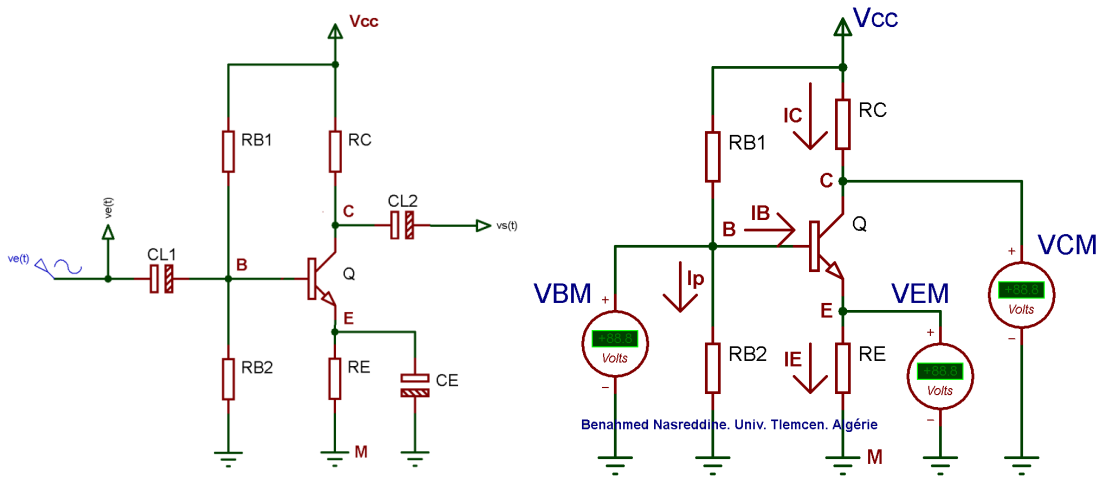

a) b)

Figure 1: Electronic schematic of a common-emitter amplifier with a decoupled emitter : in a) Dynamic mode and b) Static mode

The application of the method allows for the calculation of the following values:

- **Calculation of circuit resistances**

Component	Applied Formula	Calculated Value
Collector resistance RC	$R_C = \frac{U_T \times (-A_v)}{I_{CQ}}$	1.625 kΩ
Emitter resistance RE	$R_E = \frac{V_{EM}}{I_{CQ}}$	2.125 kΩ
Base resistance RB1	$R_{B1} = \frac{\beta(V_{CC} - V_{EM} - V_{BEQ})}{11 \times I_{CQ}}$	59.474 kΩ
Base resistance RB2	$R_{B2} = \frac{\beta(V_{EM} + V_{BEQ})}{10 \times I_{CQ}}$	33.953 kΩ

Table 1: Calculation of bias resistance values

- **Calculation of the DC voltages in the circuit**

Voltage	Applied formula	Calculated value
Emitter voltage VEM	$V_{EM} = \frac{V_{CC}}{2} + A_V \cdot U_T$	3.4 V
Base voltage VBM	$V_{BM} = V_{EM} + V_{BEQ}$	4.1 V
Collector voltage VCM	$V_{CM} = V_{CC} - I_{CQ}R_C$	9.4 V

Table 2: Calculation of DC bias voltage values

2.4 Transition from Design to Simulation and Analysis of Results

Now that the biasing resistance values for the transistor in Figure 1's circuit have been determined, we can proceed to the simulation phase to experimentally verify the amplifier's performance. This step aims to validate the theoretical design by confirming:

- The stability of the operating point.
- The accuracy of the voltage gain.
- The frequency response of the amplifier.

To achieve this, we will:

• Create the circuit schematic in Proteus;

• Verify the operating point, ensuring that ($V_{CEQ} = 6V\ et\ I_{CQ} = 1.6\,\text{mA}$);

• Analyze the frequency response and gain of the designed amplifier.

Once the design of the bipolar junction transistor (BJT) common-emitter amplifier with a decoupled emitter is completed, we proceed with experimental validation using the Proteus simulation environment. The main objective of this simulation is to ensure that the results are consistent with theoretical values, particularly the DC voltages at various circuit nodes, the voltage gain and the amplifier bandwidth.

2.4.1 Static Results

The simulation results, presented in Figure 2, show good agreement with the theoretical values obtained during the design process. Indeed, the measured voltages are:

$V_{EM} = 3.54\ ; V_{BM} = 4.23V\ ; V_{CM} = 5.76V$

These values are very close to the theoretical results, confirming a good choice of biasing resistances and a stable operating point for the transistor.

2.4.2 Dynamic Results

The responses of the designed amplifier in the time domain and frequency domain are illustrated in Figures 3 and 4.

Regarding frequency analysis, the measured gain is:

$A_v = 39.5\ dB \approx 94.4$ (linear scale).

This result is consistent with theoretical predictions, confirming the precision of the design.

The amplifier's bandwidth extends up to $f_T = 219MHz$, demonstrating good frequency response and effective amplification within the desired operating range.

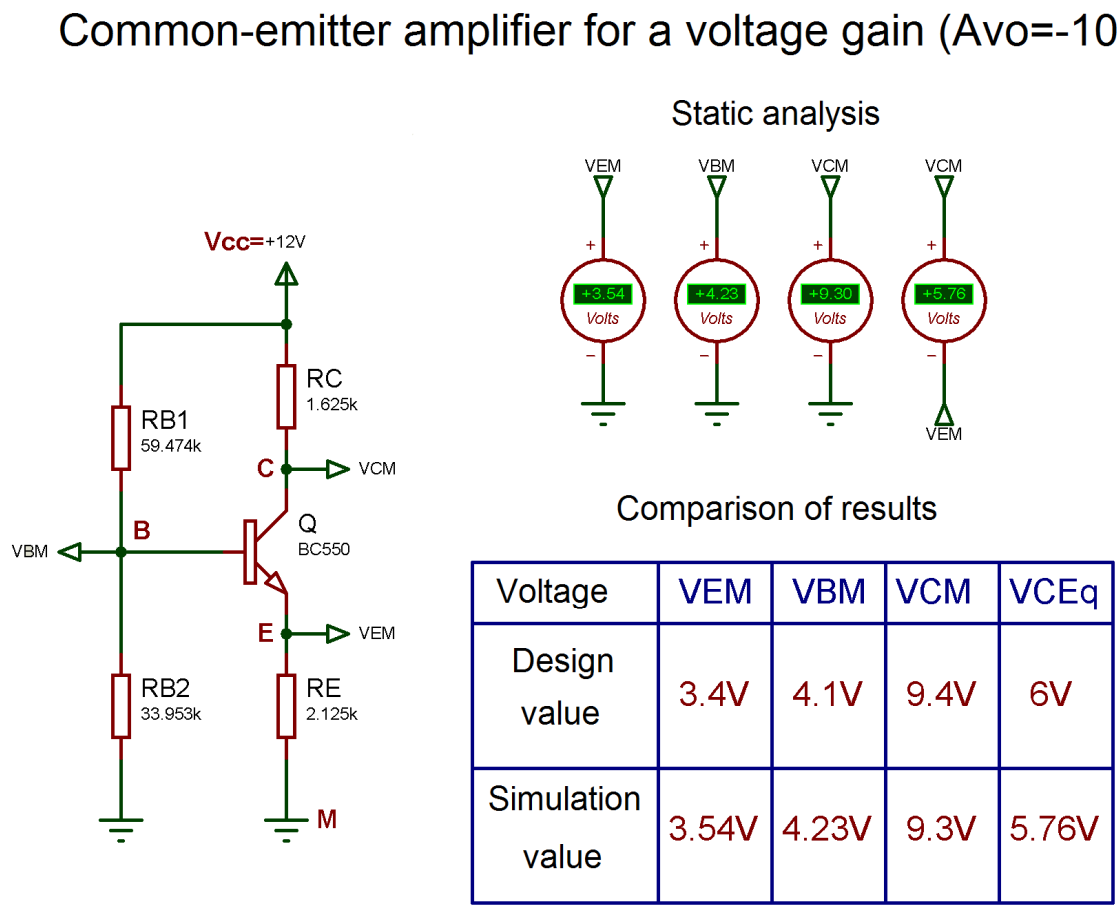

Voltage	VEM	VBM	VCM	VCEq
Design value	3.4V	4.1V	9.4V	6V
Simulation value	3.54V	4.23V	9.3V	5.76V

Figure 2: Results of the static analysis of the designed amplifier

Common-emitter amplifier for a voltage gain (Avo=-100)

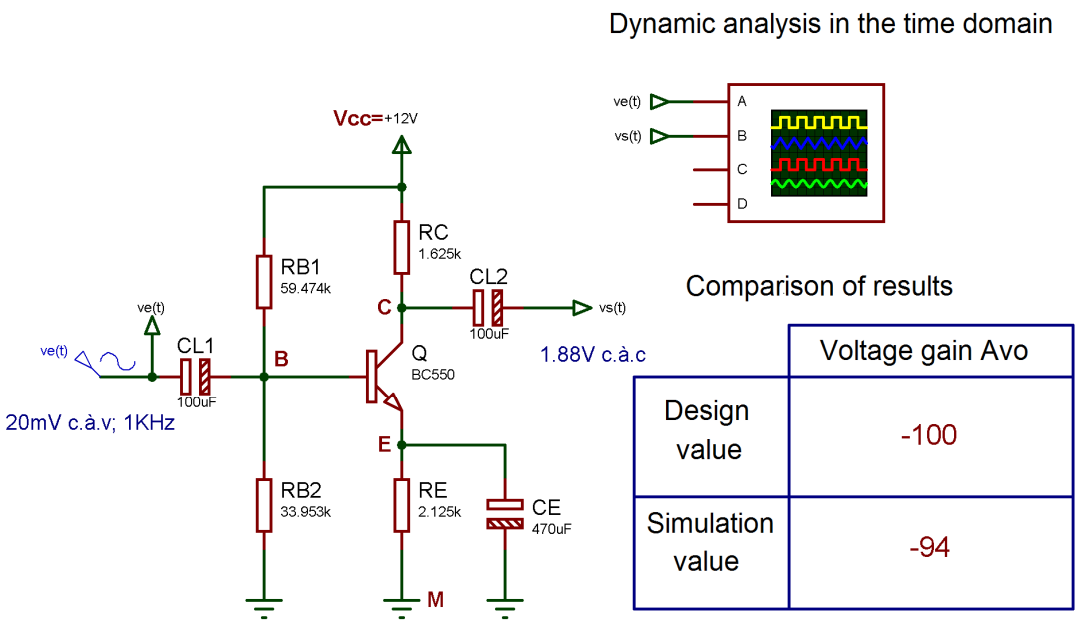

Comparison of results

	Voltage gain Avo
Design value	-100
Simulation value	-94

Figure 3: Voltage gain result of the designed amplifier

Dynamic analysis in the frequency domain

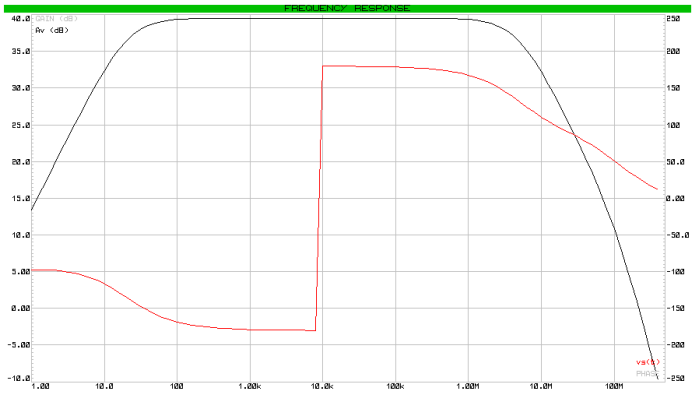

Comparison of results

	Voltage gain A_{vo}	Transition frequency f_T
Design value	-100	227.77MHz
Simulation value	-94.4	219MHz

Figure 4: Frequency response of the designed transistor amplifier.

After obtaining the frequency responses of the amplifier in Proteus, we exported the data to Excel for initial formatting, then to Origin 50 to improve the precision of the plots and obtain more readable and usable curves.

This approach allowed for a better analysis of the amplifier's frequency behavior, focusing on voltage gain A_v and phase shift Φ. Figure 5 illustrates these results with higher resolution, facilitating the interpretation of the designed amplifier's performance.

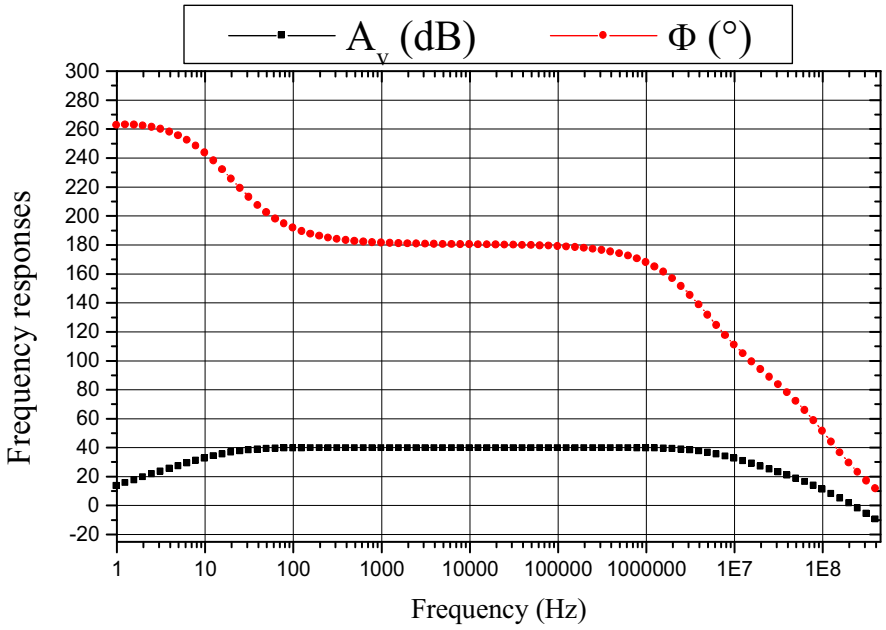

Figure 5: Plot of the frequency responses of the designed transistor amplifier in ORIGIN 50

2.5 Benahmed Method for Determining the Transfer Function of a Common-Emitter Amplifier

The Benahmed method allows for the modeling of the frequency behavior of a common-emitter (CE) amplifier with a decoupled emitter, taking into account the transistor's internal emitter capacitance C_e. This analytical approach enables precise characterization of high-frequency limitations, by defining transition and cutoff frequencies and determining the transfer function expression $A(p)$ in the Laplace domain [1, 4].

2.5.1 Determination of the Transition Frequency f_T

The transition frequency represents the frequency at which the transistor's internal capacitive effects begin to dominate and is given by:

$$f_T = \frac{I_{CQ}}{2\pi \times U_T \times C_e}$$

Where C_e is the transistor emitter capacitance.

2.5.2 Determination of the High Frequency f_h

The high frequency of the amplifier, which defines the bandwidth, is obtained from the following relation:

$$f_T = |A_v|\, f_h \;\rightarrow\; f_h = \frac{f_T}{|A_v|}$$

This expression shows that as the gain A_v increases, the bandwidth decreases.

2.5.3 Determination of the Transfer Function A(p)

The amplifier can be modeled by a rational transfer function in the Laplace domain:

$$A(p) = -\frac{|A_v|}{1 + \frac{p}{2\pi f_h}}$$

Where:

$p = j\omega$ is the Laplace variable.

f_h is the high frequency previously determined.

2.5.4 Application of the Method for $C_e = 43pF$

We will now apply this method to the designed amplifier, maintaining the same specifications as before while taking into account $Ce = 43pF$.

- **Calculation of the Transition Frequency f_T**

According to the Benahmed method, the transition frequency is given by:

$$f_T = \frac{I_{CQ}}{2\pi \times U_T \times C_e}$$

By substituting the values:

$I_{CQ} = 1.6mA$; $U_T = 26mV$; $C_e = 43pF$

$$f_T = \frac{I_{CQ}}{2\pi \times U_T \times C_e}$$

- **Calculation of the High Frequency f_h**

$$f_h = \frac{f_T}{|A_v|}$$

Avec $|A_v| = 100$:

$$f_h = \frac{228 \times 10^6}{100} = 2.28MHz$$

- **Determination of the Transfer Function A(p)**

The general expression of the transfer function is :

$$A(p) = -\frac{|A_v|}{1 + \frac{p}{2\pi f_h}}$$

By substituting $f_h = 2.28MHz$

$$A(p) = -\frac{|A_v|}{1 + \frac{p}{2\pi f_h}} = -|A_v| \times \frac{2\pi f_h}{p + 2\pi f_h} = -100 \times \frac{2\pi \times 2.28 \times 10^6}{p + 2\pi \times 2.28 \times 10^6}$$

$$\rightarrow A(p) = -100 \times \frac{1.43184 \times 10^7}{p + 1.43184 \times 10^7}$$

2.5.5 Conclusion

The application of the Benahmed method to the designed amplifier, incorporating $C_e = 43pF$, has led to the following results:

- The low-frequency gain is confirmed to be -100.
- The high cutoff frequency is approximately 2.28 MHz, defining the amplifier's bandwidth.
- The transfer function expression reveals the presence of a single pole located at f_h, which limits high-frequency response and gradually reduces the gain beyond this frequency [5].

2.6 Determination of the Transfer Function from Simulation Results in Proteus

Based on the results obtained from the Proteus simulation, we measured a transition frequency of $f_T = 219MHz$ and a low-frequency gain of $A_v \approx 94.4$.

These experimental values allow us to graphically determine the expression of the transfer function (p), taking into account the real effects of the simulated circuit.

Consequently:

$$f_h = \frac{f_T}{|A_v|} = \frac{219 \times 10^6}{94.4} = 2.32MHz$$

$$A(p) = -\frac{|A_v|}{1 + \frac{p}{2\pi f_h}} = -|A_v| \times \frac{2\pi f_h}{p + 2\pi f_h} = -94.4 \times \frac{2\pi \times 2.32 \times 10^6}{p + 2\pi \times 2.32 \times 10^6}$$

$$\rightarrow A(p) = -94.4 \times \frac{1.457 \times 10^7}{p + 1.457 \times 10^7}$$

2.7 Comparison Between the Theoretical Transfer Function and the One Obtained from Simulation

To precisely analyze the frequency response of the common-emitter (CE) amplifier with a decoupled emitter, we compare two transfer function models:

The theoretical transfer function, derived from the strict application of the Benahmed method, assuming an ideal behavior for the transistor and its components:

$$A_1(p) = -100 \times \frac{1.43184 \times 10^7}{p + 1.43184 \times 10^7}$$

The transfer function obtained from the Proteus simulation incorporates the real effects of the circuit, including parasitic elements, component tolerances, and practical limitations of the transistor:

$$A_2(p) = -94.4 \times \frac{1.457 \times 10^7}{p + 1.457 \times 10^7}$$

We will simulate and plot the frequency responses of both transfer functions, as shown in Figure 6.

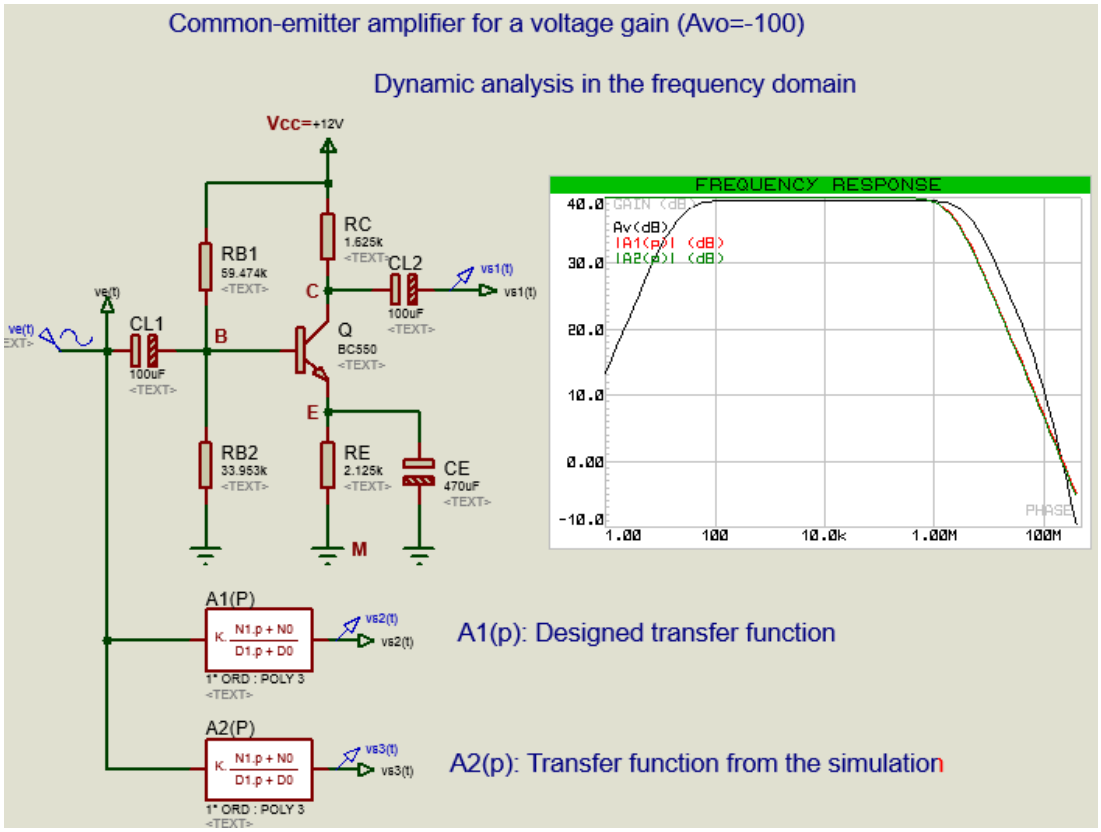

Figure 6: Simulation in PROTEUS of the designed transistor amplifier and its transfer functions in the frequency domain [6, 7]

Finally, we will compare these obtained curves with the experimental results from the real discrete transistor amplifier setup, in order to validate the accuracy of the theoretical model and assess the impact of physical imperfections.

This analysis will help optimize the amplifier's mathematical model and enhance design precision for practical applications.

2.8 Analysis and Interpretation of Frequency Responses

The analysis of Figure 7 presents three curves, illustrating the frequency responses of the designed amplifier, along with its theoretical and simulated transfer functions.

Here are the main observations:

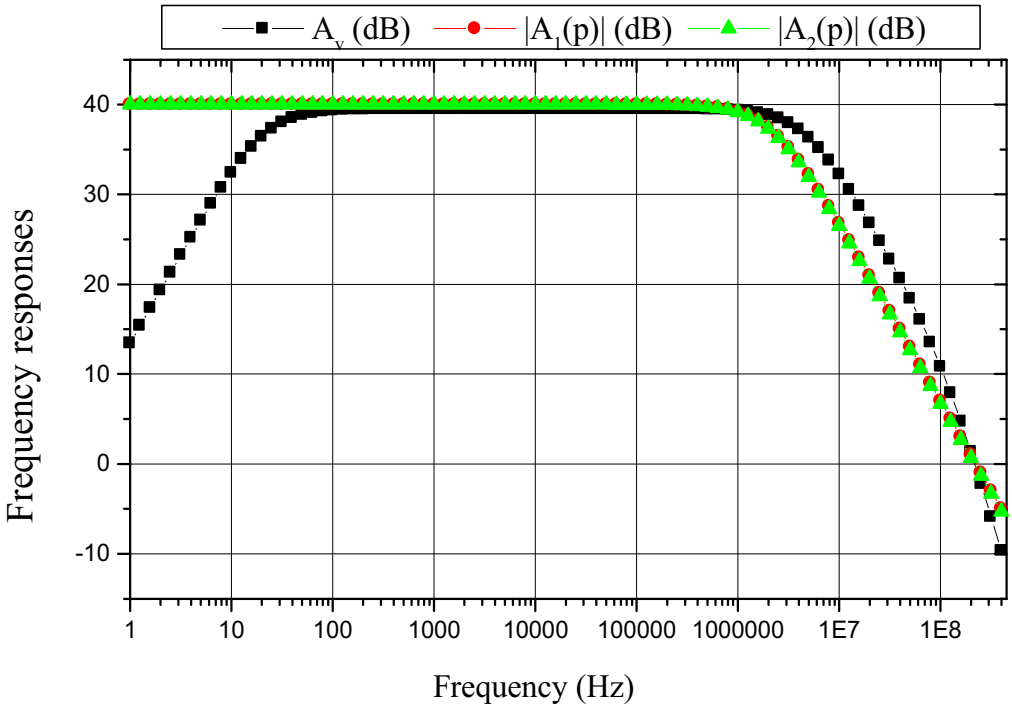

Figure 7: Plot of the frequency responses of the designed transistor amplifier in ORIGIN 50

2.8.1 Analysis of the Curves

- **Black curve (A(dB)) – Represents the actual response of the amplifier**
- This curve represents the frequency response of the actual amplifier designed in Proteus.
- A well-defined bandwidth is observed, with a stable gain at low frequencies, followed by a gradual decrease in gain beyond a certain point (high cutoff frequency).
- The decay slope reveals a behavior dominated by the transistor's internal capacitive effects.

- **Red curve ($|A_1(p)|$ in dB) – Theoretical transfer function**

- This represents the frequency response of the theoretical transfer function $A_1(p)$.
- The similarity to the experimental curve indicates that the analytical model used to derive the transfer function is relatively accurate.

- A slight difference in the transition region may be attributed to simplifications made in the theoretical model.

- **Green curve ($|A_2(p)|$ in dB) – Simulated transfer function**

- This curve corresponds to the transfer function obtained from simulation results (with $f_T = 219MHz$ and $|A_v| = A_{vo} = 94.4$).
- It is almost perfectly aligned with the theoretical curve, confirming the validity of the proposed amplifier model.

2.8.2 Comparison and Accuracy of the Model

- **Superposition of Frequency Responses**

- At low frequencies, the three curves are nearly identical, indicating that the theoretical model and simulation align well with the actual amplifier's performance.
- At high frequencies, the gain drop follows the expected trend. However, the black curve (representing the real amplifier) exhibits a slightly more gradual decay compared to the analytical models, likely due to parasitic effects not accounted for in the theoretical expression.

- **Stability of the Transition Frequency**

- The high cutoff frequency is practically identical across all curves, demonstrating a strong correlation between the real amplifier, the theoretical transfer function, and the simulated model.
- This confirms that the parameters used to derive the transfer function are consistent with the transistor's characteristics and the amplifier circuit design.

- **Validation of the Mathematical Model**

- The fact that the experimentally obtained transition frequency matches the one predicted by simulation and theoretical analysis strengthens the validity of the model used.
- The amplifier behaves as a single dominant pole system, where the bandwidth is primarily defined by the transition frequency f_T.

2.8.3 Conclusion

The analysis of the obtained curves confirms that the analytical expression of the transfer function accurately predicts the frequency response of the amplifier.

However, deviations at high frequencies may arise due to parasitic effects and model limitations. Therefore, simulation becomes essential to refine the design and validate the actual performance of the circuit.

2.9 Validation of the Theoretical Model through Time-Domain Simulation

To validate the theoretical model of the transfer function for the decoupled-emitter bipolar amplifier, a time-domain simulation was performed. This approach enables analysis of the circuit's dynamic response to an input signal, allowing for precise measurement of the voltage gain A_v.

The oscillogram presented in Figure 8 illustrates the circuit's response when subjected to a sinusoidal input signal $v_e(t)$ of 20mV amplitude at a frequency of 1 KHz. Observing the output signal $v_s(t)$, displayed in blue, reveals an amplitude of approximately 2V, corresponding to a voltage gain A_v = 100. This result is fully consistent with theoretical predictions. Additionally, the input and output signals are phase-inverted, a typical characteristic of a common-emitter amplifier.

The waveform analysis highlights a linear response from the circuit, with good preservation of the sinusoidal shape, confirming the expected behavior of the decoupled-emitter bipolar amplifier.

Thus, the obtained results validate the theoretical transfer function model of the amplifier, confirming its relevance and accuracy under the studied simulation conditions.

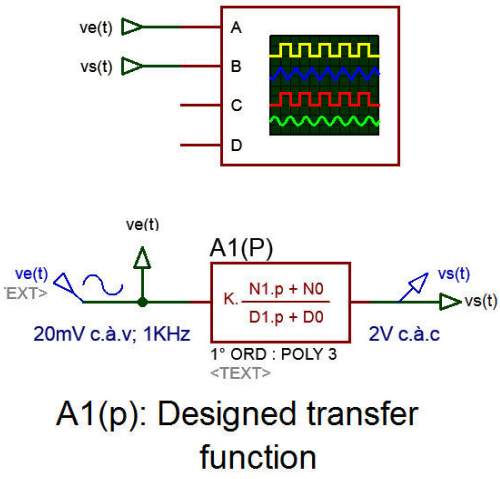

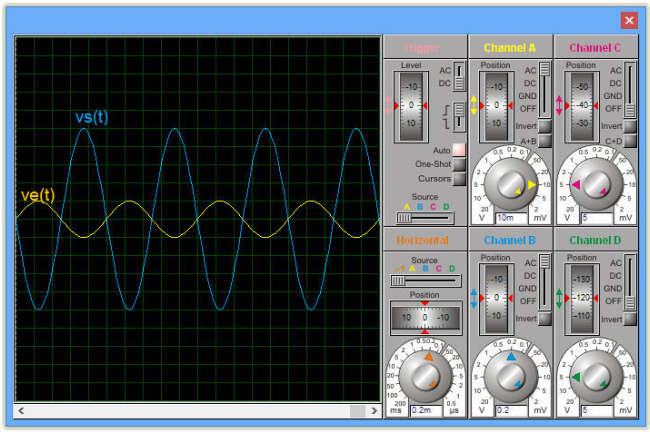

Figure 8: Simulation of the transfer function of the decoupled-emitter bipolar amplifier in the time domain

2.10 Conclusion

The results obtained from this study confirm the relevance and accuracy of the Benahmed method for the design of decoupled-emitter bipolar amplifiers.The frequency analysis demonstrated that the theoretical transfer function derived from this method closely corresponds to the simulation results in Proteus, thus validating the analytical expressions for gain and bandwidth.

Furthermore, the time-domain simulation has shown that replacing the real amplifier with its transfer function allows for an accurate reconstruction of the circuit's dynamic response, with gain and phase matching theoretical predictions.

These results highlight that the Benahmed method is a powerful tool, enabling precise determination of bias resistances, while also facilitating the development of a robust analytical model for the amplifier. However, slight deviations at high frequencies may be attributed to parasitic effects and non-ideal transistor behaviors. A more detailed study could integrate these parameters to further refine the model's accuracy and explore its application to more complex amplifiers.

Bibliographic References

[1] Benahmed, N. (2024). Our Method for Designing Bipolar Transistor Common-Emitter Amplifiers for Fixed Voltage Gain. ResearchGate. Available at: https://www.researchgate.net/publication/379342246.

[2] Sedra, A. S., & Smith, K. C. (2020). Microelectronic Circuits. Oxford University Press.

[3] Gray, P. R., Hurst, P. J., Lewis, S. H., & Meyer, R. G. (2009). Analysis and Design of Analog Integrated Circuits. Wiley.

[4] Razavi, B. (2016). Fundamentals of Microelectronics. Wiley.

[5] Millman, J., & Grabel, A. (1997). Microelectronics. McGraw-Hill.

[6] Boylestad, R. L., & Nashelsky, L. (2019). Electronic Devices and Circuit Theory. Pearson.

[7] Franco, S. (2014). Design with Operational Amplifiers and Analog Integrated Circuits. McGraw-Hill.

Chapter 3: Modeling Operational Amplifier-Based Amplifiers Using the Transfer Function

3.1 Introduction

Operational amplifiers (op-amps) are essential electronic components widely used in analog circuits for various applications, ranging from filtering to signal amplification [1]. Unlike bipolar transistor amplifiers, op-amps offer very high open-loop gain and a very high input impedance, making them ideal for low-frequency applications requiring precise and stable configurations [2].

This chapter explores the different amplifier configurations using op-amps, their modeling through transfer functions, and their simulation in Proteus 8 Professional.

3.2 Transfer Function of a Real Op-Amp

3.2.1 Definition and Expression of the Transfer Function

The study of the transfer function of operational amplifiers is fundamental in electronics, as it allows for the evaluation of their behavior depending on frequency [3]. This function, denoted as (p), is defined in the Laplace domain, where p represents the complex variable. It characterizes an op-amp's ability to amplify a signal while considering its real-world limitations [4].

The general expression of the transfer function of an operational amplifier (Figure 1) is given by:

$$A(p) = \frac{V_s(p)}{V_+(p) - V_-(p)}$$

where :

$V_s(p)$ is the output voltage expressed in the Laplace domain.

$V_+(p)\ and\ V_-(p)$ represent the voltages at the non-inverting and inverting inputs of the operational amplifier, respectively.

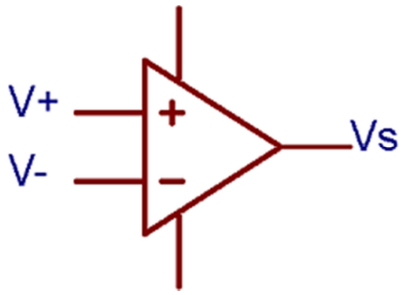

Figure 1: Electronic symbol of an op-amp

In practice, this transfer function is often modeled as a single-pole function, taking the form of a low-pass filter. For a real op-amp, it is expressed as follows [1]:

$$A(p) = \frac{A_{vo}}{1 + \frac{p}{\omega_h}} = \frac{A_{vo}\ \omega_h}{p + \omega_h}$$

where:

A_{vo} represents the open-loop gain.

ω_h denotes the high frequency or system pole.

3.2.2 Frequency Analysis and Bode Plot

The frequency response analysis of a real operational amplifier, as shown in Figure 2, is essential for understanding its behavior in a circuit. The asymptotic Bode plot of the magnitude of $A(j\omega)$ highlights two distinct regions [5]:

- When p $\ll \omega_h$, the gain is approximately constant and equal to $A_{vo\ dB}$, which results in a horizontal line on the Bode diagram.
- When p $\gg \omega_h$, the gain decreases proportionally to $\frac{1}{p}$, corresponding to a slope of -20 dB per decade [2].

The transition frequency ω_T, which corresponds to the point where the gain becomes unity ($|A(j\omega)| = 1$), is determined by the following equation :

$\omega_T = A_{vo} \times \omega_h$

This equation highlights the concept of the gain-bandwidth product, which is a key characteristic of amplifiers. Specifically, the higher the open-loop gain, the more restricted the bandwidth.

Classical operational amplifiers, such as the μA741, have a gain-bandwidth product of approximately 1 MHz, with an open-loop gain of around 2×10^5. Based on these parameters, the pole frequency can be determined using the following equation :

$$f_h = \frac{f_t}{A_{vo}}\Big|_{\mu A741} = \frac{10^6}{2 \times 10^5} = 5Hz$$

This behavior has a direct impact on circuits using an operational amplifier, limiting the frequency range over which a high gain can be maintained.

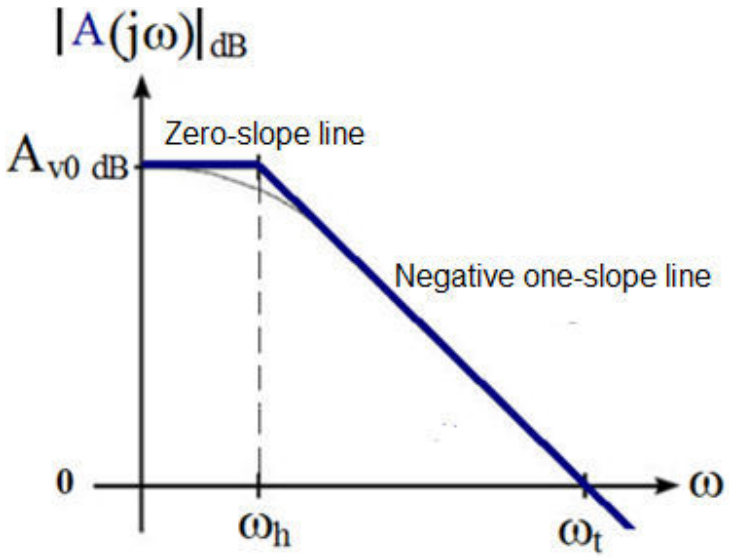

Figure 2: Asymptotic Bode representation of the magnitude of the transfer function (p) in open-loop for a real op-amp

3.3 Inverting Amplifier

3.3.1 Electronic Diagram

The inverting amplifier is one of the most common configurations using an operational amplifier. It consists of an input resistor R_1 and a feedback resistor R_2, connected as follows:

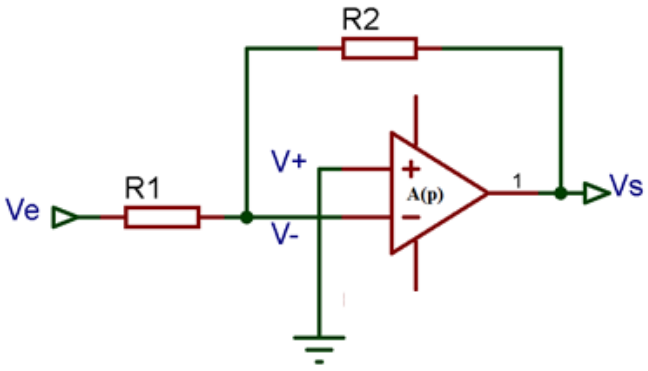

Figure 3: Circuit diagram of an inverting amplifier based on a real op-amp

• The input signal is applied to R_1, which is connected to the inverting input (-) of the op-amp.

• The non-inverting input (+) is connected to ground.

• The output is connected to R_2, which feeds back to the inverting input.

3.3.2 Determination of the Transfer Function of an Inverting Amplifier in the Laplace Domain

The analysis of the transfer function of an inverting amplifier in the Laplace domain requires consideration of the real characteristics of the operational amplifier used. Unlike an ideal model, a real operational amplifier exhibits certain limitations, such as finite gain, restricted bandwidth, and non-ideal input and output impedances.

For an inverting amplifier based on a real op-amp like the µA741, it is essential to integrate its specific parameters to achieve a more accurate representation of its behavior. Manufacturer-provided technical data, such as open-loop gain and upper cutoff frequency, must be taken into account to properly model its performance.

By applying fundamental concepts of electrical circuit analysis, it is possible to establish the expression for the transfer function of this amplifier while considering the feedback circuit components and the intrinsic properties of the operational amplifier used.

The transfer function expression for the inverting amplifier can be derived, for example, using Millman's theorem, which allows for the establishment of a mathematical relationship precisely describing the circuit's operation while accounting for the imperfections of the operational amplifier [6].

We proceed as follows:

$$A(p) = \frac{V_s(p)}{V_+(p) - V_-(p)} \rightarrow V_s(p) = -A(p)\, V_-(p)\ because\ V_+(p) = 0$$

Or :

$$V_-(p) = \frac{\frac{V_e(p)}{R_1} + \frac{V_s(p)}{R_2}}{\frac{1}{R_1} + \frac{1}{R_2}} = \frac{R_1 V_s(p) + R_2 V_e(p)}{R_1 + R_2}$$

So :

$$V_s(p) = -A(p)\frac{R_1 V_s(p) + R_2 V_e(p)}{R_1 + R_2}$$

$$\rightarrow V_s(p)\left(1 + \frac{A(p)R_1}{R_1 + R_2}\right) = -A(p)\frac{R_2 V_e(p)}{R_1 + R_2}$$

$$\rightarrow \frac{V_s(p)}{V_e(p)} = \frac{\frac{A(p)R_2}{R_1 + R_2}}{\left(1 + \frac{A(p)R_1}{R_1 + R_2}\right)} = \frac{A(p)R_2}{R_1 + R_2 + A(p)R_1}$$

$$= -\frac{R_2}{\frac{R_1 + R_2}{A(p)} + R_1} = -\frac{R_2}{1 + \left(\frac{R_1 + R_2}{R_1\, A(p)}\right)} = -\frac{\frac{R_2}{R_1}}{1 + \frac{\left(1 + \frac{R_2}{R_1}\right)}{A(p)}}$$

Finally:

$$H(p) = \frac{V_s(p)}{V_e(p)}$$

$$\rightarrow H(p) = -\frac{\frac{R_2}{R_1}}{1 + \frac{\left(1 + \frac{R_2}{R_1}\right)}{A(p)}}$$

For $p = j\omega$ and when $\left|\frac{\left(1+\frac{R_2}{R_1}\right)}{A(p)}\right| \ll 1$, the transfer function is expressed as:

$$H(p) = \frac{V_s(p)}{V_e(p)} = -\frac{R_2}{R_1}$$

This corresponds to the expression for the voltage gain of the inverting amplifier under the assumption that the operational amplifier is considered ideal.

By substituting the expression for A(p) into that of H(p), we obtain:

$$H(p) = -\frac{\frac{R_2}{R_1}}{1+\frac{\left(1+\frac{R_2}{R_1}\right)}{A(p)}} = -\frac{\frac{R_2}{R_1}}{1+\frac{\left(1+\frac{R_2}{R_1}\right)}{\frac{A_{vo}}{1+\frac{p}{\omega_h}}}} = -\frac{\frac{R_2}{R_1}}{1+\frac{\left(1+\frac{R_2}{R_1}\right)}{A_{vo}}\left(1+\frac{p}{\omega_h}\right)}$$

$$= -\frac{\frac{R_2}{R_1}}{1+\frac{\left(1+\frac{R_2}{R_1}\right)}{A_{vo}}+\frac{\left(1+\frac{R_2}{R_1}\right)}{A_{vo}}\frac{p}{\omega_h}} = -\frac{\frac{R_2}{R_1}}{\left(1+\frac{\left(1+\frac{R_2}{R_1}\right)}{A_{vo}}\right)+\left(1+\frac{\frac{\left(1+\frac{R_2}{R_1}\right)}{A_{vo}}}{1+\frac{\left(1+\frac{R_2}{R_1}\right)}{A_{vo}}}\frac{p}{\omega_h}\right)}$$

$$= -\frac{\frac{\frac{R_2}{R_1}}{\left(1+\frac{\left(1+\frac{R_2}{R_1}\right)}{A_{vo}}\right)}}{\left(1+\frac{\frac{\left(1+\frac{R_2}{R_1}\right)}{A_{vo}}}{1+\frac{\left(1+\frac{R_2}{R_1}\right)}{A_{vo}}}\frac{p}{\omega_h}\right)} = -\frac{\frac{\frac{R_2}{R_1}}{\left(1+\frac{\left(1+\frac{R_2}{R_1}\right)}{A_{vo}}\right)}}{1+\frac{p}{\frac{1+\frac{\left(1+\frac{R_2}{R_1}\right)}{A_{vo}}}{\frac{\left(1+\frac{R_2}{R_1}\right)}{A_{vo}}}\omega_h}} = -\frac{\frac{\frac{R_2}{R_1}}{\left(1+\frac{\left(1+\frac{R_2}{R_1}\right)}{A_{vo}}\right)}}{1+\frac{p}{\frac{1+\left(1+\frac{R_2}{R_1}\right)}{\left(1+\frac{R_2}{R_1}\right)}\omega_h}}$$

$$= -\frac{\frac{\frac{R_2}{R_1}}{\left(1+\frac{\left(1+\frac{R_2}{R_1}\right)}{A_{vo}}\right)}}{1+\frac{p}{\left(1+\frac{A_{vo}}{\left(\frac{R_1+R_2}{R_1}\right)}\right)\omega_h}} = -\frac{\frac{\frac{R_2}{R_1}}{\left(1+\frac{\left(1+\frac{R_2}{R_1}\right)}{A_{vo}}\right)}}{1+\frac{p}{\left(1+\frac{A_{vo}R_1}{R_1+R_2}\right)\omega_h}} = -\frac{\frac{\frac{R_2}{R_1}}{\left(1+\frac{R_1+R_2}{A_{vo}R_1}\right)}}{1+\frac{p}{\left(1+\frac{A_{vo}R_1}{R_1+R_2}\right)\omega_h}}$$

$$= \frac{-A_{v\emptyset}}{1 + \frac{p}{\omega_H}}$$

$$H(p) = \frac{V_s(p)}{V_e(p)} = -\frac{\frac{\frac{R_2}{R_1}}{\left(1 + \frac{R_1 + R_2}{A_{vo}R_1}\right)}}{1 + \frac{p}{\left(1 + \frac{A_{vo}R_1}{R_1 + R_2}\right)\omega_h}} = \frac{-A_{v\emptyset}}{1 + \frac{p}{\omega_H}}$$

With : $A_{v\emptyset} = \frac{\frac{R_2}{R_1}}{\left(1+\frac{R_1+R_2}{A_{vo}R_1}\right)}$ represents the gain of the inverting amplifier while taking into account the real characteristics of the operational amplifier.

$\omega_H = \left(1 + \frac{A_{vo}R_1}{R_1+R_2}\right)\omega_h$ corresponds to the high frequency of the inverting amplifier using a real operational amplifier.

Furthermore, the negative sign in the expression of H(p) indicates a phase opposition between the signals $v_e(t)$ and $v_s(t)$ in the time domain.

After establishing the transfer function expression for the inverting amplifier while considering the real characteristics of the operational amplifier, we can analyze it in the Laplace domain. This analysis allows us to evaluate the impact of the limitations and specificities of the real op-amp on the overall behavior of the inverting amplifier an essential aspect for the design and optimization of efficient and reliable electronic circuits.

Figure 4 illustrates the asymptotic Bode plot of the magnitude of the transfer function H(p) for the inverting amplifier using a real op-amp, derived from its expression as follows:

- When $p \ll \omega_H$, then H(p) $\rightarrow A_{v\emptyset}$, which means $|\mathrm{H(p)}|_{dB}$.

$\rightarrow 20\log(A_{v\emptyset}) = 20log\left(\frac{\frac{R_2}{R_1}}{\left(1+\frac{R_1+R_2}{A_{vo}R_1}\right)}\right)$ representing a horizontal line (zero slope).

- When $p \gg \omega_H$, then H(p) $\rightarrow \frac{A_{v\emptyset}\,\omega_H}{p}$, corresponding to a line with a slope of -1.

$|\mathrm{H(p)}|_{dB} = 0$ which means $|\mathrm{H(p)}| = 1 \rightarrow p_T = A_{v\emptyset}\,\omega_H = \frac{\frac{R_2}{R_1}}{\left(1+\frac{R_1+R_2}{A_{vo}R_1}\right)}\left(1+\frac{A_{vo}R_1}{R_1+R_2}\right)\omega_h$

$\cong \frac{R_2}{R_1}\left(1+\frac{A_{vo}R_1}{R_1+R_2}\right)\omega_h \cong \frac{R_2}{R_1}\frac{A_{vo}R_1}{R_1+R_2}\omega_h \cong \frac{R_2}{R_1+R_2}A_{vo}\omega_h$

$\cong \frac{R_2}{R_1+R_2}\omega_t = \omega_T < \omega_t$

Thus, the transition angular frequency ω_T of the inverting amplifier using a real operational amplifier differs from the transition angular frequency ω_t of the real op-amp itself. This contrasts with the case of a non-inverting amplifier with a real op-amp, where these two frequencies coincide.

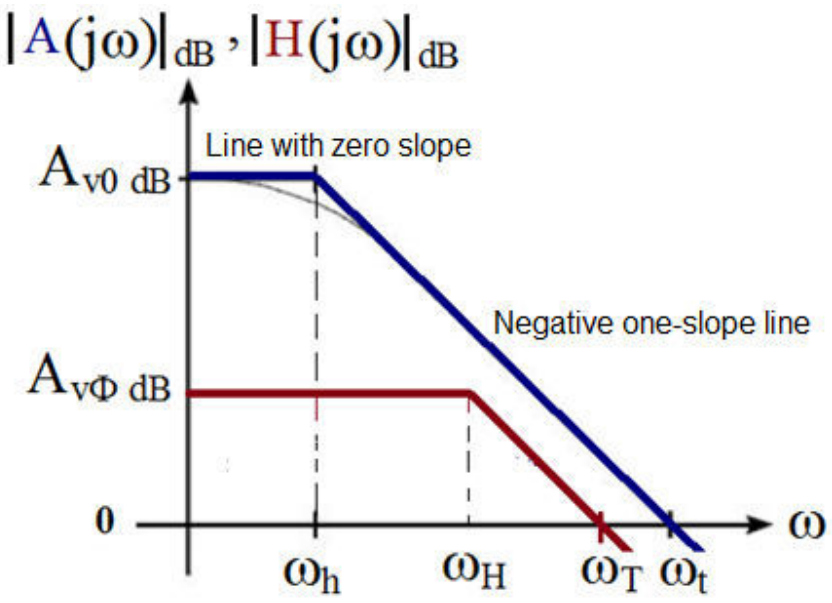

Figure 4: Influence of finite gain and bandwidth on the frequency response of the inverting amplifier with a real op-amp

In this concrete example from Figure 5, we analyze an inverting amplifier consisting of specific resistances ($R_1 = 1K\Omega\ et\ R_2 = 33K\Omega$) along with the operational amplifier µA741. The theoretical results, obtained from previously established equations, will be compared with simulation results performed in the Proteus environment.

3.3.3 Simulation in Proteus

Figure 5, extracted from the µA741 datasheet, illustrates the evolution of the magnitude of its open-loop transfer function A(p) as a function of frequency.

The typical value of the open-loop voltage gain is:

$A_{v0} = A_{vd} = 2 \times 10^5$

which corresponds, in decibels, to:

$A_{v0\,dB} = 20\log(2 \times 10^5) = 106dB$

The gain-bandwidth product, corresponding to the transition frequency of the µA741, is given by:

$f_t = 1MHz$

Thus, the high-frequency limit is calculated as follows:

$$f_h = \frac{\omega_h}{2\,\pi} = \frac{f_t}{A_{v0}} = \frac{10^6}{2 \times 10^5} = 5Hz$$

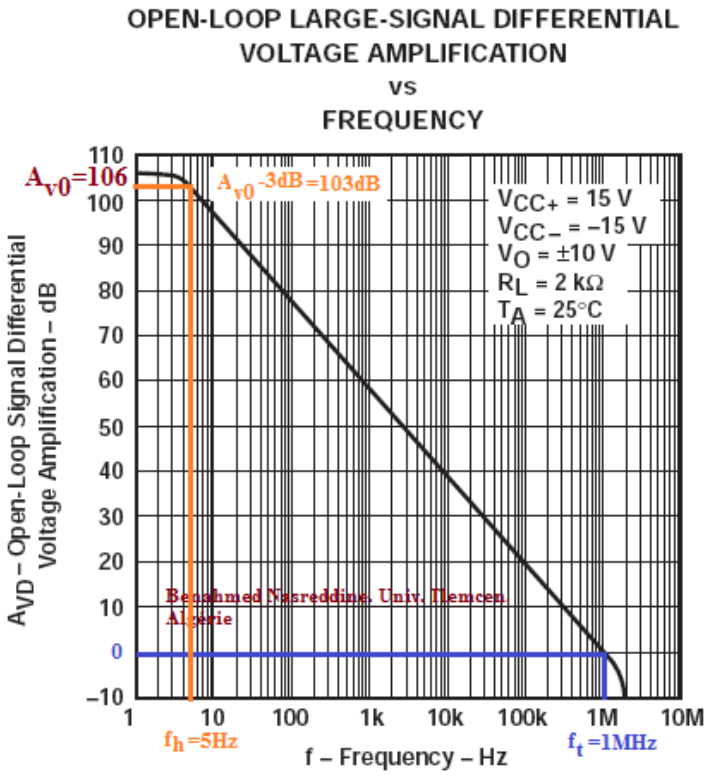

Figure 5: Evolution of the magnitude of the open-loop transfer function A(p) for the µA741 [4]

- **Theoretical Results**

For the given resistance values ($R_1 = 1K\Omega$ and $R_2 = 33K\Omega$), the theoretical gain of the inverting amplifier shown in Figure 3 is approximately 33. Indeed:

$$R_1 = 1K\Omega \; et \; R_2 = 33K\Omega \rightarrow A_{v\emptyset} = \frac{\frac{R_2}{R_1}}{\left(1+\frac{R_1+R_2}{R_1 A_{v0}}\right)} = \frac{\frac{33}{1}}{\left(1+\frac{1+33}{1\times 2\times 10^5}\right)} = \frac{33}{(1+17\times 10^{-5})} = 32.994 \approx 33$$

Furthermore, the theoretical gain-bandwidth product, corresponding to the transition frequency f_T of this inverting amplifier, is given by:

$$f_T \cong \frac{R_2}{R_{1+}R_2} f_t = \frac{33}{34} \times 10^6 = 970.6KHz.$$

Meanwhile, its upper cutoff frequency (bandwidth) is:

$$f_H = \left(1 + \frac{A_{v0}\, R_1}{R_1+R_2}\right) f_h = \left(1 + \frac{2\times 10^5 \times 1}{1+33}\right) \times 5 = 29.42KHz$$

- **Simulation Results in Proteus**

To verify the validity of the model $A(p)|_{\mu A741} = \frac{2\times 10^5}{1+318.47\times 10^{-4}\, p}$, established for the µA741 operational amplifier in the first chapter, we compared its frequency response to that provided by the manufacturer (Figure 5). For this purpose, a frequency response simulation of our model was performed in the Proteus environment (Figure 6). The obtained results confirm that our model accurately describes the behavior of the µA741, as they align with the manufacturer's frequency response data.

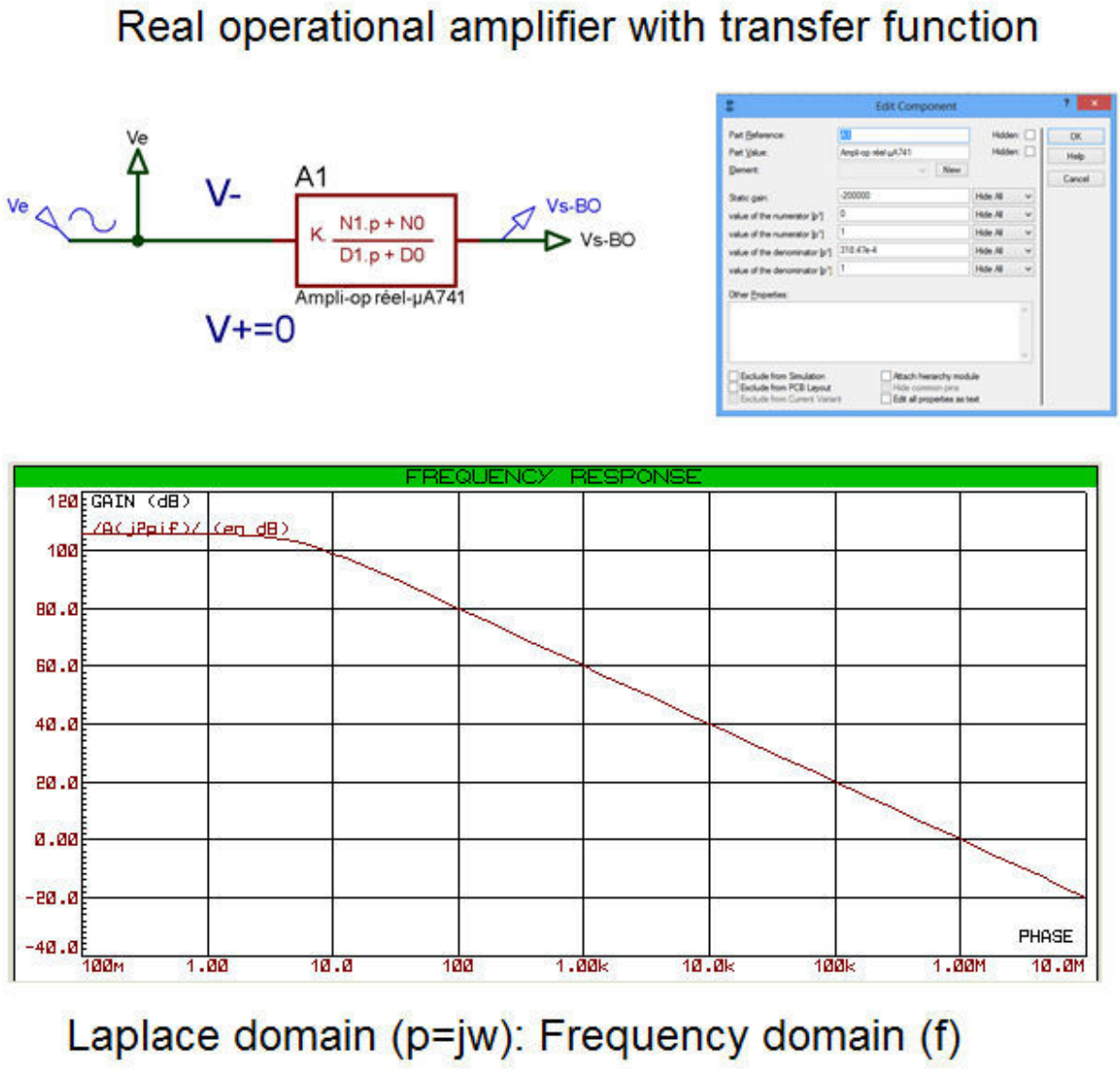

Figure 6: Frequency response simulation of the model A(p) for the µA741 operational amplifier in Proteus 8 Professional

We then integrated the transfer function A(p) with discrete components R_1 and R_2 to construct an inverting amplifier, as illustrated in Figure 7. This circuit combines the open-loop transfer function A(p) of the µA741 operational amplifier with the resistances $R_1 = 1K\Omega$ et $R_2 = 33\ K\Omega$ [7].

Inverting amplifier with the transfer function of the µA741

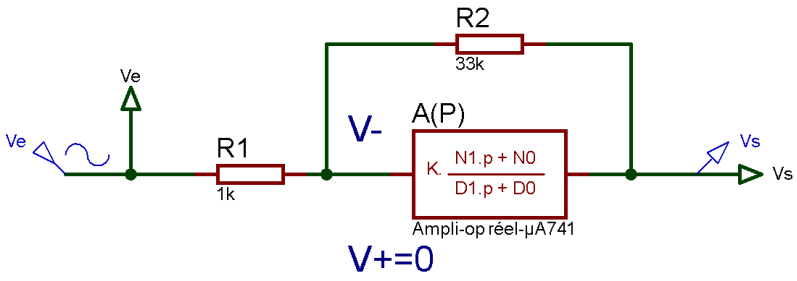

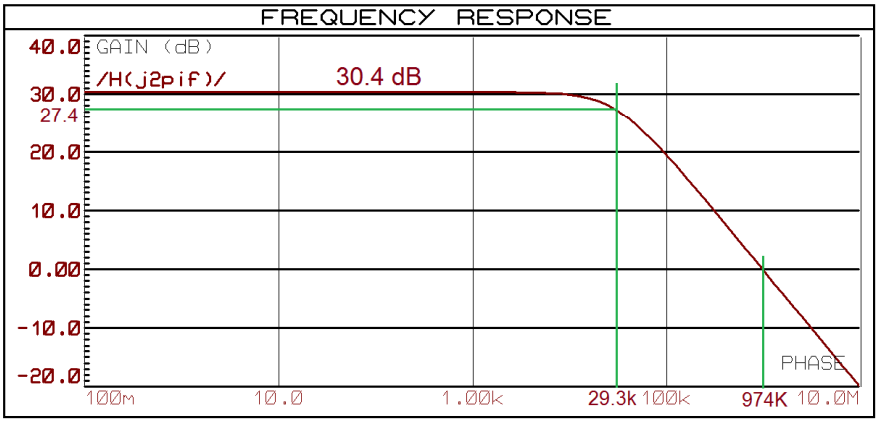

Laplace domain (p=jw): Frequency domain (f)

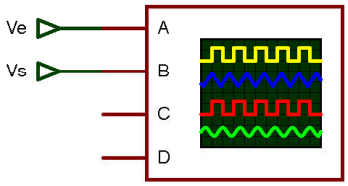

Time domain (t)

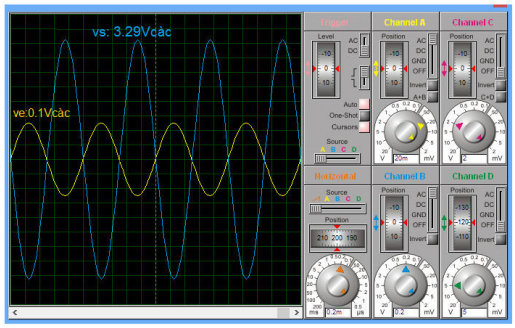

Figure 7: Frequency and time response of an inverting amplifier based on the µA741 with its transfer function

The analysis of the results obtained from the simulation of the inverting amplifier circuit based on the transfer function of the µA741 operational amplifier leads to several conclusions:

- **Frequency Response**

The gain curve in decibels (dB) indicates that the inverting amplifier maintains a constant gain of approximately 30 dB within the useful bandwidth, which is consistent with the theoretical amplification factor:

$$A_v = -\frac{R_2}{R_1} = -\frac{33}{1} = -33\ (about\ 30.4dB)$$

Beyond the frequency $f_{\mathrm{H}} = 29.3\ KHz$ (obtained at -3dB, i.e., 30.4 - 3 = 27.4dB) and up to the transition frequency $f_T = 974\ KHz$, the gain starts to decrease, which is consistent with the typical frequency response of an inverting amplifier using the µA741 op-amp. This behavior is due to bandwidth limitations and the internal compensation of the µA741.

- **Time-Domain Analysis**

➢ The oscilloscope displays the input $v_{\mathrm{e}}(t)$ in yellow and the output $v_s(t)$ in blue.

➢ The observed amplification is consistent with the expected factor, meaning the output signal $v_s(t)$ is amplified by a factor of $-\frac{3.29}{0.1} = -32.9$ compared to $v_{\mathrm{e}}(t)$, which means a 180° phase inversion.

➢ The waveform analysis confirms the proper functioning of the circuit in the time domain, with no visible distortion within the tested frequency range (f = 1KHz).

- **General Interpretation**

➢ The inverting amplifier circuit designed using the transfer function of the µA741 operational amplifier performs as expected in terms of gain and frequency response.

➢ The inverting amplifier, based on the transfer function of the µA741, operates in line with theoretical expectations, maintaining correct gain, phase shift, and frequency response.

➢ The observed high-frequency limitations are consistent with the characteristics of the μA741, which has a relatively narrow closed-loop bandwidth ($f_{\mathrm{H}} = 29.3\ KHz$).

➢ Due to its well-defined transfer function, this configuration is primarily suitable for applications requiring linear amplification with phase inversion, particularly for low-frequency signals, where the frequency limitations of the μA741 ($ft = 1\ MHz$) compared to the BC550 transistor ($f_T \approx 228MHz$) are not a major constraint.

3.4 Conclusion on the Inverting Amplifier

The study conducted on the inverting amplifier based on the μA741 operational amplifier allowed for an analysis of its transfer function, considering the real characteristics of the component. The theoretical approach, derived from Laplace-domain transfer function equations, was validated through Proteus simulations, confirming the consistency between the obtained results and the manufacturer's specifications.

The frequency-domain analysis revealed a stable gain within the useful bandwidth, with a roll-off consistent with the high-frequency limitations of the μA741. The time-domain study, on the other hand, demonstrated an amplification behavior faithful to theoretical predictions, exhibiting the characteristic 180° phase inversion of this configuration

However, high-frequency performance remains limited due to the restricted gain-bandwidth product of the μA741 operational amplifier. Optimizing the transfer function could enable better utilization in applications requiring a wider bandwidth. This section of the chapter thus paves the way for the study of other operational amplifiers that offer more suitable performance for high-frequency applications.

3.5 Non-Inverting Amplifier

3.5.1 Circuit Diagram

The non-inverting amplifier is a widely used configuration with an operational amplifier (Figure 8). It consists of an input resistor and a feedback resistor, connected as follows:

- The input signal is applied to the non-inverting input (+) of the operational amplifier.
- The inverting input (−) is connected to a portion of the output signal via a voltage divider formed by the feedback resistors.

• The output of the operational amplifier is connected to the feedback network to stabilize the gain of the circuit.

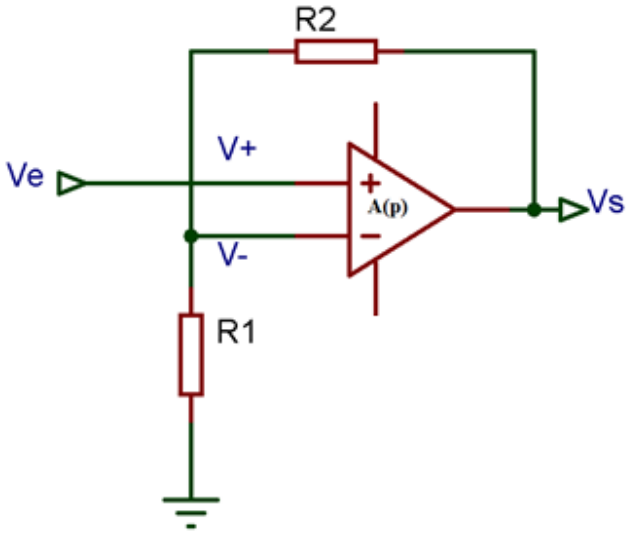

Figure 8: Circuit diagram of a non-inverting amplifier based on a real operational amplifier

3.5.2 Determination of the Transfer Function of a Non-Inverting Amplifier in the Laplace Domain

The analysis of the transfer function of a non-inverting amplifier in the Laplace domain requires consideration of the real parameters of the operational amplifier used. Unlike the ideal model, a real operational amplifier exhibits limitations such as finite gain, restricted bandwidth, and non-ideal input and output impedances.

In the case of a non-inverting amplifier using a real operational amplifier such as the µA741, it is crucial to incorporate its specific characteristics to achieve a more precise modeling. The parameters provided by the manufacturer, including open-loop gain and cutoff frequency, must be taken into account to accurately represent its behavior.

By applying the fundamental principles of electrical circuit analysis, the transfer function of this amplifier can be expressed in terms of the feedback circuit elements and the intrinsic characteristics of the operational amplifier.

The transfer function expression of the configuration can be derived, for instance, by applying the feedback equations, thereby establishing a precise mathematical relationship that describes its operation while accounting for the imperfections of the operational amplifier [8].

We proceed as follows:

$$V_+(p) = V_e(p) \; and \; V_-(p) = \frac{R_1}{R_1 + R_2} V_s(p)$$

Or:

$$A(p) = \frac{V_s(p)}{V_+(p) - V_-(p)} \leftrightarrow V_s(p) = A(p) \left[V_e(p) - \frac{R_1}{R_1 + R_2} V_s(p) \right]$$

$$\leftrightarrow V_s(p) = A(p) V_e(p) - \frac{R_1}{R_1 + R_2} A(p) V_s(p)$$

$$\leftrightarrow \left[1 + \frac{R_1}{R_1 + R_2} A(p) \right] V_s(p) = A(p) V_e(p)$$

$$\rightarrow \frac{V_s(p)}{V_e(p)} = \frac{A(p)}{1 + \frac{R_1}{R_1 + R_2} A(p)} = \frac{A(p)}{\frac{R_1}{R_1 + R_2} \left[\frac{R_1 + R_2}{R_1} + A(p) \right]} = \frac{\frac{R_1 + R_2}{R_1} A(p)}{\frac{R_1 + R_2}{R_1} + A(p)} = \frac{1 + \frac{R_2}{R_1}}{1 + \frac{\left(1 + \frac{R_2}{R_1}\right)}{A(p)}}$$

Finally :

$$H(p) = \frac{V_s(p)}{V_e(p)} = \frac{1 + \frac{R_2}{R_1}}{1 + \frac{\left(1 + \frac{R_2}{R_1}\right)}{A(p)}}$$

For $p = j\omega$ and when $\left| \frac{\left(1 + \frac{R_2}{R_1}\right)}{A(p)} \right| \ll 1$, the transfer function is expressed as:

$$H(p) = \frac{V_s(p)}{V_e(p)} = 1 + \frac{R_2}{R_1}$$

This corresponds to the voltage gain expression of the non-inverting amplifier, assuming the operational amplifier is considered ideal.

By substituting the expression of A(p) into that of H(p), we obtain:

$$H(p)=\frac{1+\frac{R_2}{R_1}}{1+\frac{\left(1+\frac{R_2}{R_1}\right)}{A(p)}}=\frac{1+\frac{R_2}{R_1}}{1+\frac{\left(1+\frac{R_2}{R_1}\right)}{\frac{A_{vo}}{1+\frac{p}{\omega_h}}}}=\frac{1+\frac{R_2}{R_1}}{1+\frac{\left(1+\frac{R_2}{R_1}\right)}{A_{vo}}\left(1+\frac{p}{\omega_h}\right)}$$

$$=\frac{1+\frac{R_2}{R_1}}{1+\frac{\left(1+\frac{R_2}{R_1}\right)}{A_{vo}}+\frac{\left(1+\frac{R_2}{R_1}\right)}{A_{vo}}\frac{p}{\omega_h}}=\frac{1+\frac{R_2}{R_1}}{\left(1+\frac{\left(1+\frac{R_2}{R_1}\right)}{A_{vo}}\right)\left(1+\frac{\frac{\left(1+\frac{R_2}{R_1}\right)}{A_{vo}}\frac{p}{\omega_h}}{1+\frac{\left(1+\frac{R_2}{R_1}\right)}{A_{vo}}}\right)}$$

$$=\frac{\frac{1+\frac{R_2}{R_1}}{\left(1+\frac{\left(1+\frac{R_2}{R_1}\right)}{A_{vo}}\right)}}{\left(1+\frac{\frac{\left(1+\frac{R_2}{R_1}\right)}{A_{vo}}\frac{p}{\omega_h}}{1+\frac{\left(1+\frac{R_2}{R_1}\right)}{A_{vo}}}\right)}=\frac{\frac{1+\frac{R_2}{R_1}}{\left(1+\frac{\left(1+\frac{R_2}{R_1}\right)}{A_{vo}}\right)}}{1+\frac{p}{\frac{1+\frac{\left(1+\frac{R_2}{R_1}\right)}{A_{vo}}}{\frac{\left(1+\frac{R_2}{R_1}\right)}{A_{vo}}}\omega_h}}=\frac{\frac{1+\frac{R_2}{R_1}}{\left(1+\frac{\left(1+\frac{R_2}{R_1}\right)}{A_{vo}}\right)}}{1+\frac{p}{\frac{A_{vo}+\left(1+\frac{R_2}{R_1}\right)}{\left(1+\frac{R_2}{R_1}\right)}\omega_h}}$$

$$=\frac{\frac{1+\frac{R_2}{R_1}}{\left(1+\frac{\left(1+\frac{R_2}{R_1}\right)}{A_{vo}}\right)}}{1+\frac{p}{\left(1+\frac{A_{vo}}{\frac{R_1+R_2}{R_1}}\right)\omega_h}}=\frac{\frac{1+\frac{R_2}{R_1}}{\left(1+\frac{\left(1+\frac{R_2}{R_1}\right)}{A_{vo}}\right)}}{1+\frac{p}{\left(1+\frac{A_{vo}R_1}{R_1+R_2}\right)\omega_h}}=\frac{\frac{1+\frac{R_2}{R_1}}{\left(1+\frac{R_1+R_2}{A_{vo}R_1}\right)}}{1+\frac{p}{\left(1+\frac{A_{vo}R_1}{R_1+R_2}\right)\omega_h}}$$

$$H(p)=\frac{A_{v\emptyset}}{1+\frac{p}{\omega_H}}$$

With: $A_{v\emptyset} = \frac{1+\frac{R_2}{R_1}}{\left(1+\frac{R_1+R_2}{A_{vo}R_1}\right)}$ represents the gain of the non-inverting amplifier, taking into account the real characteristics of the operational amplifier.

$\omega_H = \left(1 + \frac{A_{vo}R_1}{R_1+R_2}\right)\omega_h$ corresponds to the high-frequency limit of the non-inverting amplifier using a real operational amplifier.

In the case of the non-inverting amplifier, the absence of a negative sign in the expression of H(p) indicates that the signals $v(t)$ et $v_s(t)$ are in phase in the time domain.

After determining the transfer function expression of the non-inverting amplifier, considering the real characteristics of the operational amplifier, we can proceed with its analysis in the Laplace domain. This study allows us to evaluate the impact of the real operational amplifier's limitations on the overall behavior of the amplifier, which is a key factor for the design and optimization of electronic circuits that provide stable and accurate amplification.

Figure 9 illustrates the asymptotic Bode plot of the magnitude of the transfer function H(p) for the non-inverting amplifier using a real operational amplifier, obtained from its theoretical expression

- When $p \ll \omega_H$, then $\mathrm{H}(p) \rightarrow A_{v\emptyset}$ i.e., $|H(p)|_{dB}$.

$\rightarrow 20\log(A_{v\emptyset}) = 20\log\left(\frac{1+\frac{R_2}{R_1}}{\left(1+\frac{R_1+R_2}{A_{vo}R_1}\right)}\right)$ representing a straight line with zero slope.

- When $p \gg \omega_H$, then $\mathrm{H}(p) \rightarrow \frac{A_{v\emptyset}\,\omega_H}{p}$, corresponding to a straight line with a slope of -1.

$|\mathrm{H}(p)|_{dB} = 0$ i.e., $H(p) = 1 \rightarrow\ p_T = A_{v\emptyset}\,\omega_H = \left(\frac{1+\frac{R_2}{R_1}}{\left(1+\frac{R_1+R_2}{A_{vo}R_1}\right)}\right)\left(1 + \frac{A_{vo}R_1}{R_1+R_2}\right)\omega_H$

$\cong \left(1 + \frac{R_2}{R_1}\right)\left(1 + \frac{A_{vo}R_1}{R_1+R_2}\right)\omega_H \cong \frac{R_1+R_2}{R_1}\frac{A_{vo}R_1}{R_1+R_2}\omega_H \cong A_{v\emptyset}\,\omega_H = \omega_T = \omega_t$

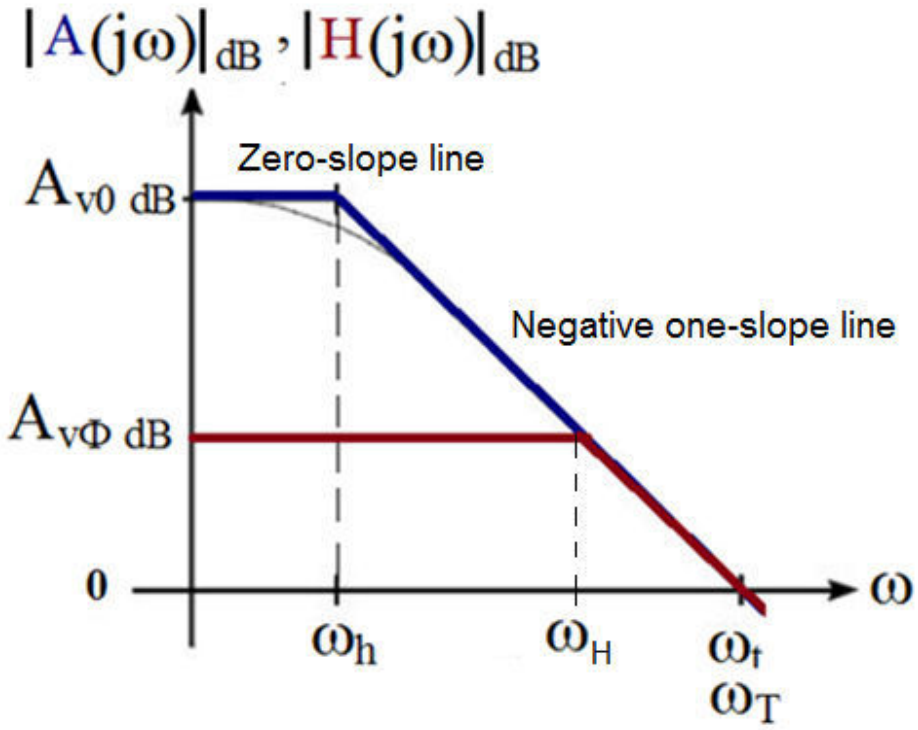

Figure 9: Influence of limited gain and bandwidth on the frequency response of the non-inverting amplifier with a real operational amplifier

Thus, the transition frequency ω_T of the non-inverting amplifier with a real operational amplifier is approximately equal to the transition frequency ω_t of the operational amplifier used.

3.5.3 Simulation in Proteus

In this concrete example illustrated in Figure 5, we study a non-inverting amplifier using specific resistances ($R_1 = 1K\Omega \; et \; R_2 = 33K\Omega$) as well as the operational amplifier µA741. The theoretical results, derived from previously established equations, will be compared with the simulation results obtained in the Proteus environment.

- **Theoretical Results**

For the given resistor values ($R_1 = 1K\Omega \; et \; R_2 = 33K\Omega$), the theoretical gain of the non-inverting amplifier shown in Figure 8 is approximately 34. Indeed:

$$R_1 = 1K\Omega \; and \; R_2 = 33K\Omega \; \rightarrow A_{v\emptyset} = \frac{1 + \frac{R_2}{R_1}}{\left(1 + \frac{R_1 + R_2}{A_{vo}R_1}\right)} = \frac{1 + \frac{33}{1}}{\left(1 + \frac{1 + 33}{1 \times 2 \times 10^5}\right)}$$

$$= \frac{34}{(1 + 17 \times 10^{-5})} = 33.994 \cong 34.$$

Moreover, the theoretical gain-bandwidth product, corresponding to the transition frequency f_T of this non-inverting amplifier, is given by:

$$f_T \cong \left(1 + \frac{R_2}{R_1}\right)\left(1 + \frac{A_{v0}R_1}{R_1 + R_2}\right) f_h \cong \left(1 + \frac{33}{1}\right)\left(1 + \frac{2 \times 10^5 \times 1}{1 + 33}\right) 5$$

$$f_T \cong 1000170Hz \cong 1MHz$$

Whereas its high frequency (bandwidth) is:

$$f_H = \left(1 + \frac{A_{v0}R_1}{R_1 + R_2}\right) f_h = \left(1 + \frac{2 \times 10^5 \times 1}{1 + 33}\right) \times 5 = 29.416KHz = \frac{10^6}{34} = \frac{f_T}{A_{v\emptyset}}$$

- **Simulation Results in Proteus**

We then implemented the transfer function A(p) using discrete components R_1 and R_2 to design a non-inverting amplifier, as illustrated in Figure 10. This circuit integrates the transfer function A(p) of the µA741 operational amplifier in open-loop configuration along with the resistances $R_1 = 1K\Omega$ et $R_2 = 33K\Omega$.

Non-inverting amplifier with transfer function

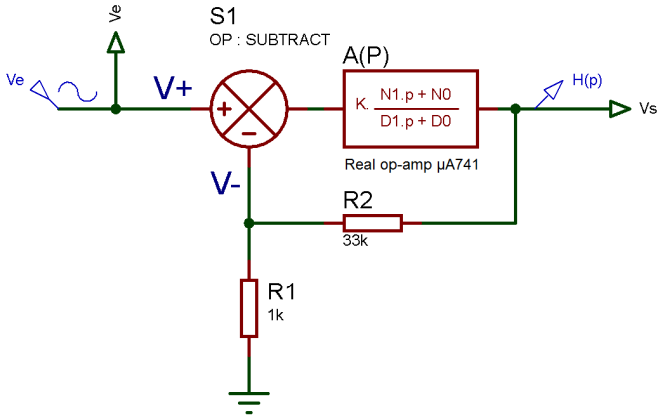

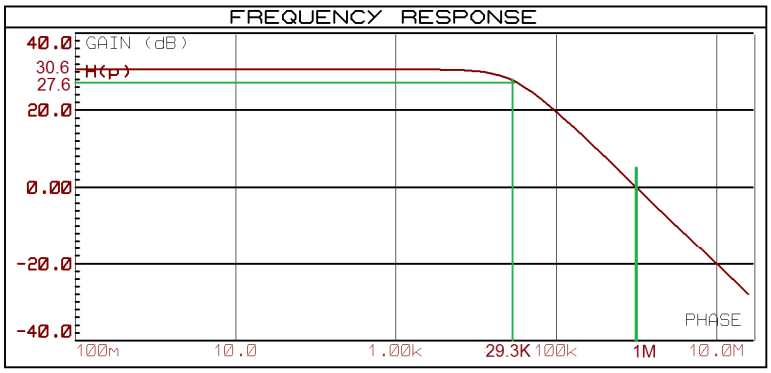

Laplace domain (p=jw): Frequency domain (f)

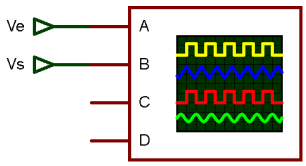

Time domain (t)

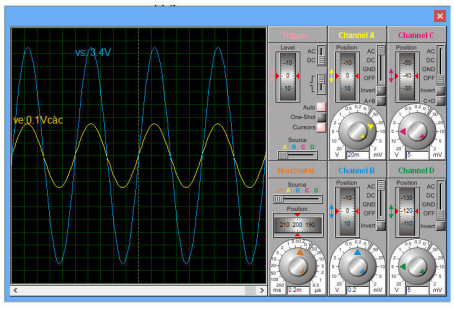

Figure 10: Frequency and time response of a non-inverting amplifier based on the µA741 with its transfer function

The analysis of the results obtained from the simulation of the non-inverting amplifier circuit, based on the transfer function of the µA741 operational amplifier, leads to several observations. Notably, the transition frequency ($f_T = 1MHz$) of the non-inverting amplifier is equal to the transition frequency ($f_t = 1MHz$) of the operational amplifier, confirming the expected behavior of the µA741 in a closed-loop configuration.

- **Frequency Response**

The analysis of the gain in decibels (dB) shows that the non-inverting amplifier maintains a constant gain of approximately 30.6 dB within the useful bandwidth. This gain is consistent with the theoretical relationship given by:

$$A_v = 1 + \frac{R_2}{R_1} = 1 + \frac{33}{1} = 34$$

This corresponds to approximately 30.63 dB.

Beyond the high cutoff frequency $f_H = 29.3\,KHz$, the gain gradually starts to decrease, illustrating bandwidth limitations and the internal compensation of the µA741. This decline is consistent with the typical behavior of operational amplifiers in closed-loop configurations, where bandwidth decreases as gain increases.

- **Time Domain Analysis**

- The oscilloscope displays the input $v_e(t)$ in yellow and the output $v_s(t)$ in blue.
- Unlike the inverting amplifier, the output is in phase with the input signal.
- The amplitude of $v_s(t)$ is amplified by a factor of $\frac{3.4}{0.1} = 34$, which corresponds to the expected theoretical values.
- The waveforms confirm the proper operation of the circuit in the time domain, without significant distortion within the tested frequency range (here f = 1KHz). The absence of noticeable distortion validates the assumption of a linear behavior of the circuit within this frequency range.

- **General Interpretation**

The non-inverting amplifier based on the transfer function of the µA741 operates as expected. It exhibits:

- A gain consistent with theoretical values.
- A frequency response limited by the bandwidth of the μA741.
- Linear amplification without phase inversion

This configuration is well-suited for applications requiring amplification without signal inversion, particularly for low-frequency signals. However, the bandwidth limitation remains a factor to consider, especially for applications that require a broader high-frequency response.

3.6 Conclusion on the Non-Inverting Amplifier

The analysis of the non-inverting amplifier using the μA741 operational amplifier has made it possible to evaluate its transfer function while incorporating the real characteristics of the component. The theoretical equations derived from Laplace domain analysis were compared with the simulation results in Proteus, highlighting a strong correlation with the manufacturer's specifications.

The frequency analysis revealed a stable gain within the useful bandwidth, with a gradual attenuation at higher frequencies, in accordance with the limitations of the μA741. The time-domain examination also confirmed amplification consistent with theoretical expectations, without phase inversion, which is an essential property of this configuration.

However, high-frequency performance remains limited due to the constrained gain-bandwidth product of the μA741. Optimizing the transfer function could enhance its efficiency for applications requiring a wider bandwidth. This study thus opens the perspective of exploring other operational amplifiers that are better suited to the requirements of high-frequency systems.

3.7 General Conclusion

This chapter explored inverting and non-inverting amplifiers, using the transfer function as a fundamental analysis tool. The study highlighted the importance of this mathematical approach in precisely characterizing the behavior of operational amplifiers, particularly the μA741, while accounting for its real-world limitations.

The frequency analysis, based on the transfer function, demonstrated the impact of the gain-bandwidth product on the frequency response of amplifiers. The inverting amplifier exhibited phase inversion, whereas the non-inverting amplifier maintained amplification without inversion, with a transition frequency equal to that of the operational amplifier.

The time-domain study, also guided by the transfer function, confirmed the agreement between theoretical results and simulations in Proteus. This consistency validates the effectiveness of the transfer function in predicting and understanding circuit behavior.

However, the performance of the amplifiers remains limited by the characteristics of the μA741, particularly at high frequencies. Optimizing the transfer function could extend their application to systems requiring a wider bandwidth. This work thus highlights the importance of the transfer function as a key tool for the design and improvement of electronic circuits.

Bibliographic References

[1] A. S. Sedra & K. C. Smith (2018). Microelectronic Circuits (8th ed.). Oxford University Press.

[2] S. Franco (2015). Design with Operational Amplifiers and Analog Integrated Circuits (4th ed.). McGraw-Hill.

[3] R. Boylestad & L. Nashelky (2020). Electronic Devices and Circuit Theory (11th ed.). Pearson.

[4] Texas Instruments (2000). µA741 Operational Amplifier Datasheet.

[5] J. Millman & A. Grabel (2017). Microelectronics (2nd ed.). McGraw-Hill.

[6] N. Benahmed & N. Benabdallah (2024). Exploration of Inverting Amplifiers Using Transfer Functions of Real Operational Amplifiers. ResearchGate. Available at: https://www.researchgate.net/publication/379079365_Exploration_des_Amplificateurs_Inverseurs_a_l'aide_de_Fonctions_de_Transfert_d'Amplificateurs_Operationnels_Reels

[7] N. Benahmed & N. Benabdallah (2024). Simulation Method for Circuits Combining Discrete Components and Transfer Functions in Proteus 8 Professional: Case of Inverting Amplifier with µA741 Op-Amp. ResearchGate. Available at: https://www.researchgate.net/publication/378857177_Methode_de_simulation_de_circuits_combinant_des_composants_discrets_et_des_fonctions_de_transfert_sous_Proteus_8_Professional_Cas_d'amplificateur_inverseur_a_ampli-op_A741

[8] N. Benahmed & N. Benabdallah (2024). Chapter Q – Non-Inverting Amplifier with Real Operational Amplifier: Non-Inverting Amplifier with Finite Gain and Bandwidth. ResearchGate. Available at: https://www.researchgate.net/publication/360972592_Chapitre_Q-Amplificateur_non_inverseur_a_AOP_reel-_Non-Inverting_amplifier_with_finite_gain_and_bandwidth

Chapter 4: Design and Simulation of a High-Frequency Virtual Bipolar Transistor in Proteus

4.1 Introduction

In modern electronics, the design of high-frequency transistors is crucial for developing fast and efficient circuits. To analyze and optimize the behavior of an NPN bipolar transistor intended for ultra-high-frequency (UHF) applications, a systematic approach to modeling and simulation is required.

In this chapter, we outline the approach taken to develop a virtual NPN transistor model, aiming for a transition frequency f_T of 1 GHz under a fixed collector current condition of $I_C = I_{CQ} = 1.6mA$.

Based on experimentally obtained results and extracted parameters, we refined a custom SPICE model in Proteus while ensuring that previously validated simulation outcomes remained consistent [1-2].

A customized SPICE model was designed in Proteus in alignment with the predefined performance objectives [3]. The parameters were meticulously adjusted to achieve the targeted characteristics during simulations.

This study not only illustrates the fundamental principles of high-frequency modeling for an active component but also highlights the constraints and trade-offs necessary to achieve the desired performance within a simulation environment.

4.2 Modeling Strategy

4.2.1 Description of SPICE Parameters

The parameters contained within a SPICE model are fundamental values that characterize the behavior of a transistor in simulation. Below is a detailed explanation of the key terms used in the .lib SPICE file for an NPN transistor model [1-2]:

- **I_S (reverse saturation current)**

Description: The reverse saturation current (I_S) is the base current that flows through the transistor when it is in the reverse saturation region. It determines the transistor's

speed and its sensitivity to temperature variations.

Typical Value: 1×10^{-14}A for a standard transistor.

- **$B_F = \beta_F$ (Base Current Gain)**

Description: β_F is the direct current gain of the transistor in the active region. It represents the ratio between the collector current (I_C) and the base current (I_B). It is a key factor in determining the transistor's performance at high frequencies.

Typical Value: 200 (meaning the transistor amplifies the base current by a factor of 200).

- **V_{AF} (Early Voltage)**

Description: V_{AF}, or Early Voltage, characterizes the depletion effect. It influences the variation of β_F as a function of the collector-emitter voltage. A higher V_{AF} value indicates a transistor with improved performance at high frequencies.

Typical Value: 50V.

- **I_{KF} (Base Saturation Injection Current)**

Description: I_{KF} represents the saturation effect in the base-emitter junction of the transistor, influencing the input characteristic curve under strong bias conditions. This parameter is used to model the variation of current gain as a function of the collector current.

Typical Value: 0.3A

- **I_{SE} (Inverse Saturation Current of the Base-Emitter Junction)**

Description: I_{SE} is the inverse saturation current at the base-emitter junction, which plays a role in modeling leakage currents at low temperatures.

Typical Value: 1×10^{-13} A.

- **N_E (Ideal Factor for the Base)**

Description: N_E represents the ideality factor in the SPICE model for the base-emitter junction. This factor helps to model deviations from the ideal diode behavior.

Typical Value: 1.5.

- **β_R (Reverse Current Gain)**

Description : β_R is the reverse current gain, representing the transistor's gain when the collector current becomes negative. It helps model nonlinear behaviors in the inverse saturation region.

Typical Value: 3.

- **N_R (Ideality Factor for the Collector-Base Junction)**

Description: N_R is the ideality factor of the collector-base junction. This parameter helps model current losses caused by the effects of the junction between the collector and the base.

Typical Value: 1.5.

- **R_B (Base Resistance)**

Description: R**B** is the internal resistance of the base junction, which influences the transistor's dynamic response at high frequencies. It plays a significant role in switching speed performance.

Typical value: 100 Ω.

- **R_C (Collector Resistance)**

Description: R_C is the internal resistance of the collector. It affects voltage drop and the transistor's bandwidth at high frequencies.

Typical value: 100 Ω.

- **R_E (Emitter Resistance)**

Description: R_E is the internal resistance of the emitter, which also influences thermal stability and the transistor's linearity.

Typical value: 1 Ω.

- **C_{JE} (Base-Emitter Junction Capacitance)**

Description: C_{JE} is the capacitance of the base-emitter junction. It has a significant impact on the transistor's high-frequency performance, particularly on the transition frequency f_T.

Typical value: 4 pF.

- **V_{JE} (Base-Emitter Junction Depletion Voltage)**

Description: V_{JE} is the depletion voltage for the base-emitter junction. This value is important for determining the variation of the C_{JE} capacitance depending on the applied voltage.

Typical value: 0.5 V.

- **C_{JC} (Collector-Base Junction Capacitance)**

Description: C_{JC} is the capacitance of the collector-base junction. It also influences the high-frequency performance of the transistor, particularly regarding the charge storage capacity.

Typical value: 2 pF.

- **V_{JC} (Collector-Base Junction Depletion Voltage)**

Description: V_{JC} is the depletion voltage for the collector-base junction. Like V_{JE}, this value affects the variation of the C_{JC} capacitance depending on the applied voltage.

Typical value: 0.5 V.

- **T_F (Base-Collector Transit Time)**

Description: T_F is the transit time, which measures the transistor's response speed. A shorter transit time helps increase the transition frequency (f_T).

Typical value: 0.1 ns.

- **T_R (Rise Time)**

Description: T_R is the rise time, which refers to the time required for the transistor's output to transition from a low to a high state.

Typical value: 10 ns.

Once these parameters are properly defined and adjusted, they enable the creation of a realistic transistor model in Proteus 8. These adjustments are essential for simulating and optimizing the transistor's behavior in high-frequency applications [4].

4.2.2 Selection of Critical Parameters

To achieve a transition frequency f_T of 1 GHz under a collector bias set at $I_C = I_{CQ} = 1.6mA$, a meticulous selection of SPICE parameters was necessary.

The main objective was to optimize the high-frequency performance of the virtual transistor that we aim to design in Proteus 8.

The parameters considered critical for directly influencing f_T are:

• The junction capacitances C_{JE} and C_{JC}, which influence the transistor's capacitive behavior at high frequencies.

• The transit time T_F, which determines the transistor's response speed.

• The direct current gain β_F (parameter B_F), which governs the device's dynamics in the active region.

• The transistor's internal resistances (not to be confused with external bias resistances) R_B, R_C et R_E, which affect bandwidth and model stability.

These parameters were prioritized for precise adjustments during the modeling phase in Proteus.

4.2.3 Adjustment of SPICE Model Parameters

Before defining the .lib file, an initial theoretical estimation of the transition frequency f_T was conducted to guide the adjustment of critical parameters.

The transition frequency f_T of a bipolar transistor can be approximated using the following equation:

$$f_T = \frac{1}{2\pi\left(\frac{C_{JE} + C_{JC}}{g_m} + T_F\right)}$$

Where :

• g_m is the transconductance, given by :

$$g_m = \frac{I_C}{V_T}$$

with $\boldsymbol{V_T}$ being the thermal voltage (approximately 26 mV at 300K).

Preliminary Calculation

For $I_C = I_{CQ} = 1.6\ m$A:

$$g_m = \frac{1.6 \times 10^{-3}}{26 \times 10^{-3}} = 0.0615\ S$$

By setting initial values : C_{JE} = 4 pF, C_{JC} = 2 pF et T_F = 0.1 ns, we can estimate the time constant :

$$\tau = \frac{(C_{JE} + C_{JC})}{g_m} + T_F = \frac{(4+2) \times 10^{-12}}{0.0615} + 0.1 \times 10^{-9} = 97.56\, ps + 100\, ps$$
$$= 197.56\, ps$$

So :

$$f_T = \frac{1}{2\pi \times 197.56 \times 10^{-12}} \approx 806\, MHz$$

This initial theoretical calculation shows that, to reach $f_T = 1\, GHz$, an additional adjustment of the transit time T_F is required.

A second quick calculation yields the following for $f_T = 1\, GHz$:

$$T_F \approx \frac{1}{2\pi \times f_T} \approx \frac{1}{2\pi \times 10^9} \approx 159\, ps$$

Given the selected capacitances, T_F needs to be slightly reduced below 0.1 ns or C_{JE} et C_{JC} must be adjusted accordingly.

Final Selection of Parameters for SPICE Modeling:

- C_{JE} = 1.63pF
- C_{JC} = 2pF
- T_F = 0.1ns
- β_F = 200 (a sufficient value to ensure good current gain)
- R_B = 100 Ω (base)
- R_C = 100 Ω (collector)
- R_E = 1 Ω (emitter)

4.2.4 Implementation of the SPICE Model

The corresponding SPICE model is:

```
MODEL BC550_FAST NPN (
+ IS=1E-14 BF=200 VAF=50 IKF=0.3 ISE=1E-13
+ NE=1.5 BR=3 NR=1.5 RB=100 RC=100 RE=1
+ CJE=1.63p VJE=0.5 CJC=2p VJC=0.5
```

+ TF=0.1n TR=10n)

Where:

IS = 1E-14; Reverse saturation current

BF = 200; Current gain in active mode

VAF = 50; Early voltage (voltage dependence model)

IKF = 0.3; High-frequency gain factor

ISE = 1E-13; High-temperature reverse saturation current

NE = 1.5; Emission factor for the base junction

BR = 3; Current gain in saturation mode

NR = 1.5; Emission factor for the collector junction

RB = 100 Ω; Base resistance

RC = 100 Ω; Collector resistance

RE = 1 Ω; Emitter resistance

CJE = 1.63 pF; Base-emitter junction capacitance (Farad)

VJE = 0.5 V; Base-emitter junction voltage

CJC = 2 pF; Collector-base junction capacitance (Farad)

VJC = 0.5 V; Collector-base junction voltage

TF = 0.1 ns; Transit time (seconds)

TR = 10 ns; Rise time (seconds)

4.2.5 Conclusion

In this section, we have detailed the process of creating a custom transistor for Proteus, including the generation of the .lib file. We have explained each step involved in defining the pins, internal architecture, and necessary parameters to build an accurate representation of the component. This part of the work enhances the Proteus library with tailor-made components, adapted to the specific requirements of simulation

The integration of the .lib file and simulation verification will be covered in the next step to ensure the validity and full functionality of the component within the design environment.

4.3 Quick Procedure for Implementing the .lib File in Proteus

To integrate a custom transistor (e.g., BC550_FAST) into Proteus from a .lib file (which should be placed in the Proteus project directory), a simple and efficient method involves using an existing symbol or creating a new one.

Here is the detailed procedure:

1- Using an Existing Symbol

- ✓ Open Proteus.
- ✓ Go to **Library → Pick Devices/Symbols**.
- ✓ Search for a standard symbol such as **NPN** or **PNP**.
- ✓ Select a symbol that matches the desired transistor type (in this case, NPN).
- ✓ This method speeds up the process without requiring the creation of a custom symbol.

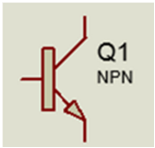

2- Linking the .lib File with Make Device

✓ Go to Library (or right-click) → Make Device.

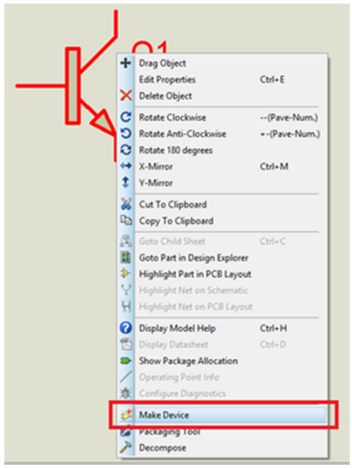

✓ In the Device Creation Wizard:

- Assign a name to the component (e.g., NPN).

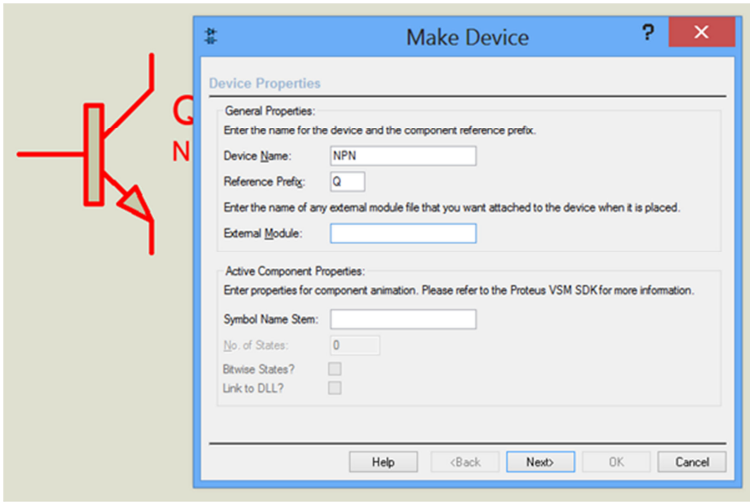

- Click Next.

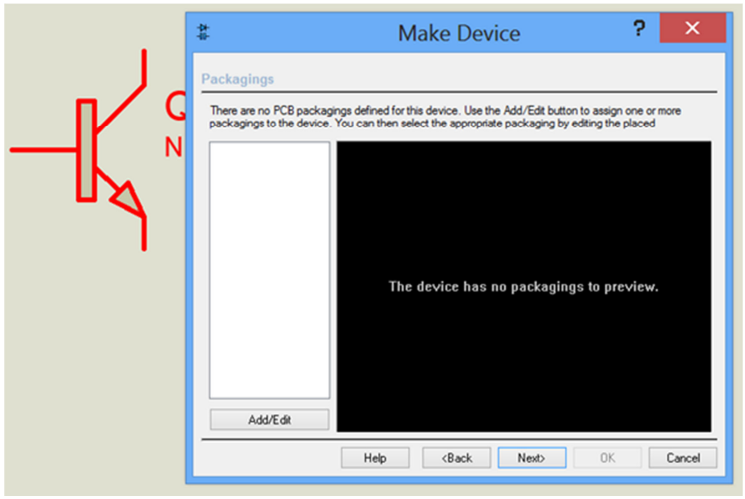

- Click Next again.

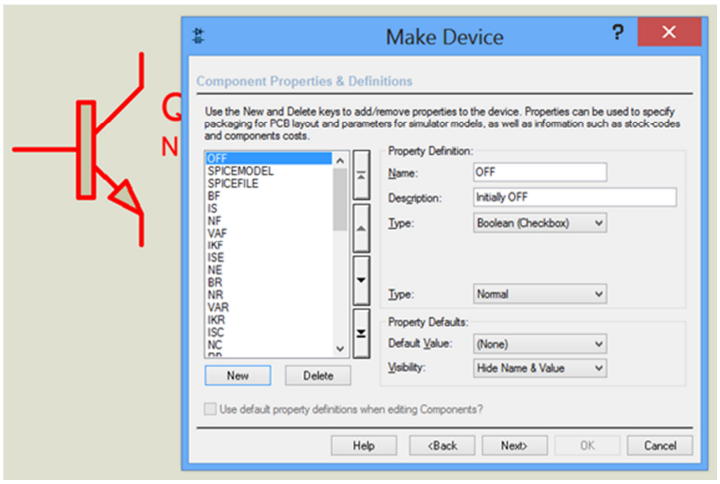

- To insert transistor parameter values, click SPICEFILE, then enter the name of the .lib file (Here, BC550_FAST.lib) as shown.

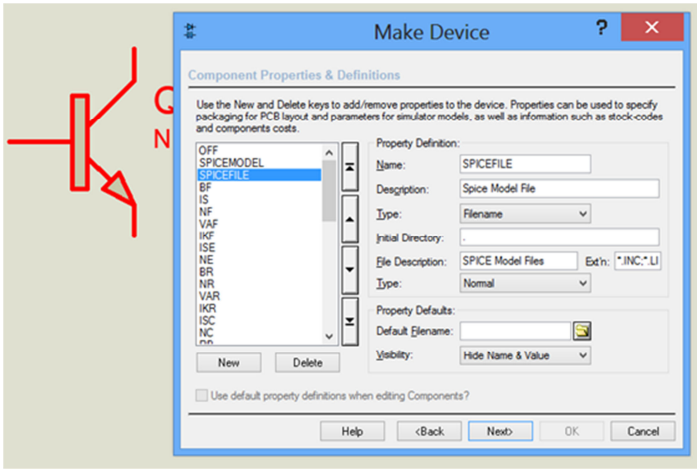

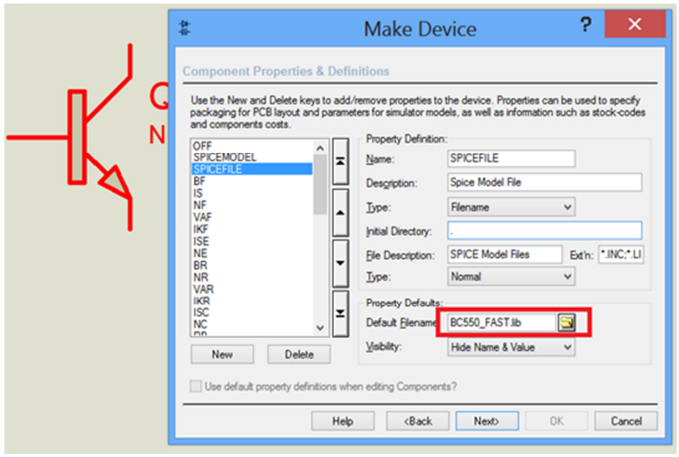

- Next, click SPICEMODEL, then enter the name that appears on the first line of the .lib file (Here, BC550_FAST) as displayed.

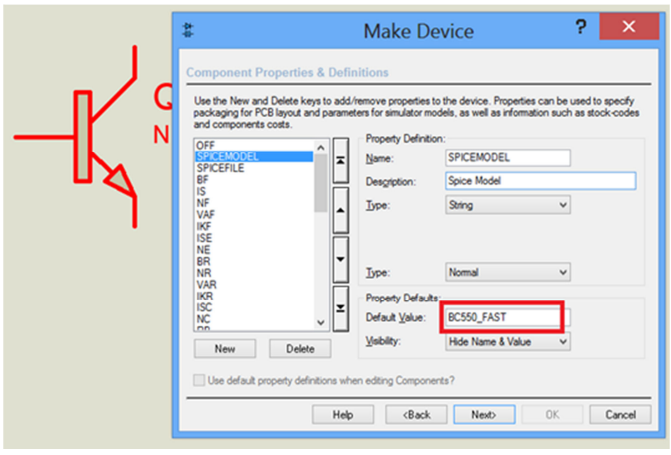

- Click Next.

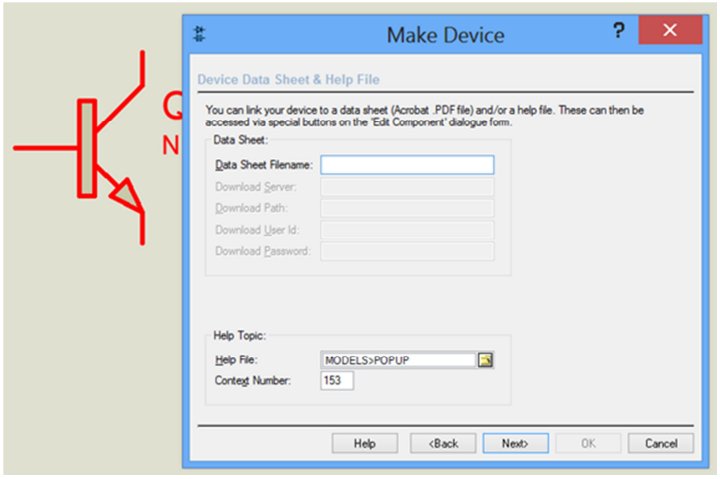

- Click Next again.

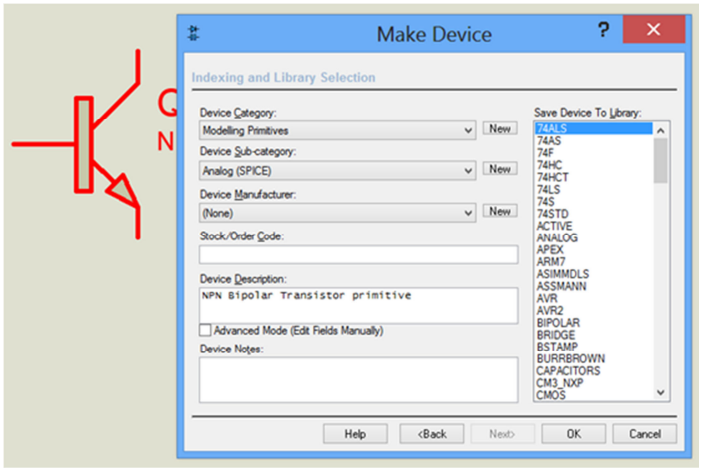

- Enter the data and finalize by clicking OK.

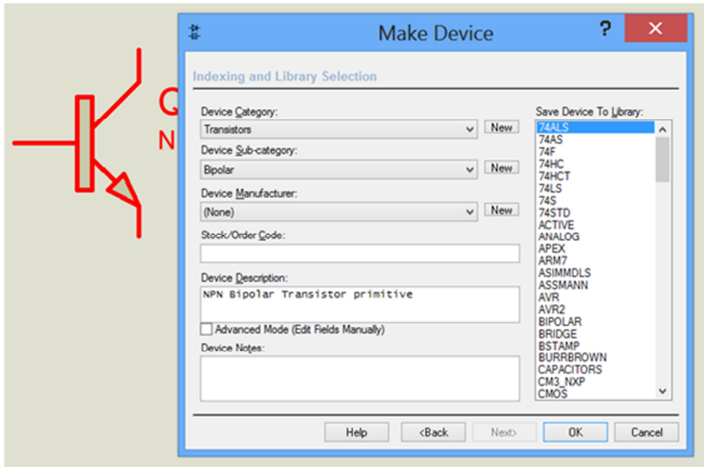

Thus, we have created a transistor called NPN within the Proteus library. This transistor incorporates parameters extracted from the .lib file, some of which were specifically defined to achieve a transition frequency f_T=1 GHz [5].

4.4 Presentation and Validation of the Model in Proteus

The practical validation of the transistor model we designed was carried out in two main steps:

4.4.1 Static Biasing of the Transistor and Dynamic Operation

First, we inserted the custom transistor into a biasing circuit, using exactly the same resistance values as those determined earlier in chapter 2.

The objective was to position the operating point (Q) at the center of the static load line, ensuring optimal linear amplification with a voltage gain of $A_v = -100$.

After simulation in Proteus, the results obtained for the static voltages (Figure 1) were identical to those previously obtained with the standard transistor from the Proteus library (see Chapter 2), this confirms the validity of the component's static modeling.

For the dynamic results (Figure 2), the measured voltage gain is:

$$A_v|_{f=1\,MHz} = -\frac{1.75}{20\times10^{-3}} = -87.5$$

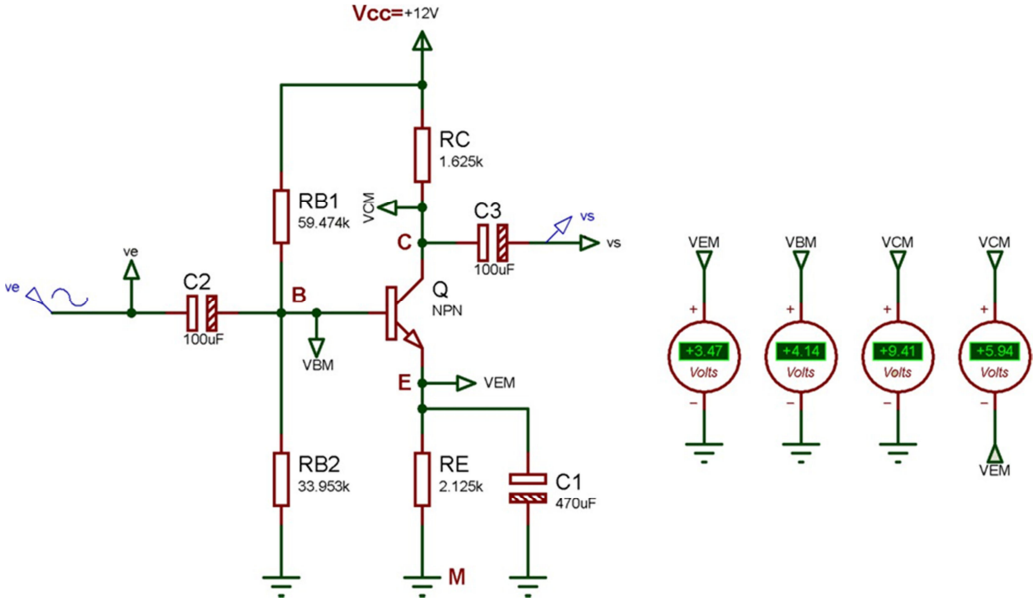

Figure 1: Static results of a common-emitter amplifier with a decoupled emitter using our custom transistor

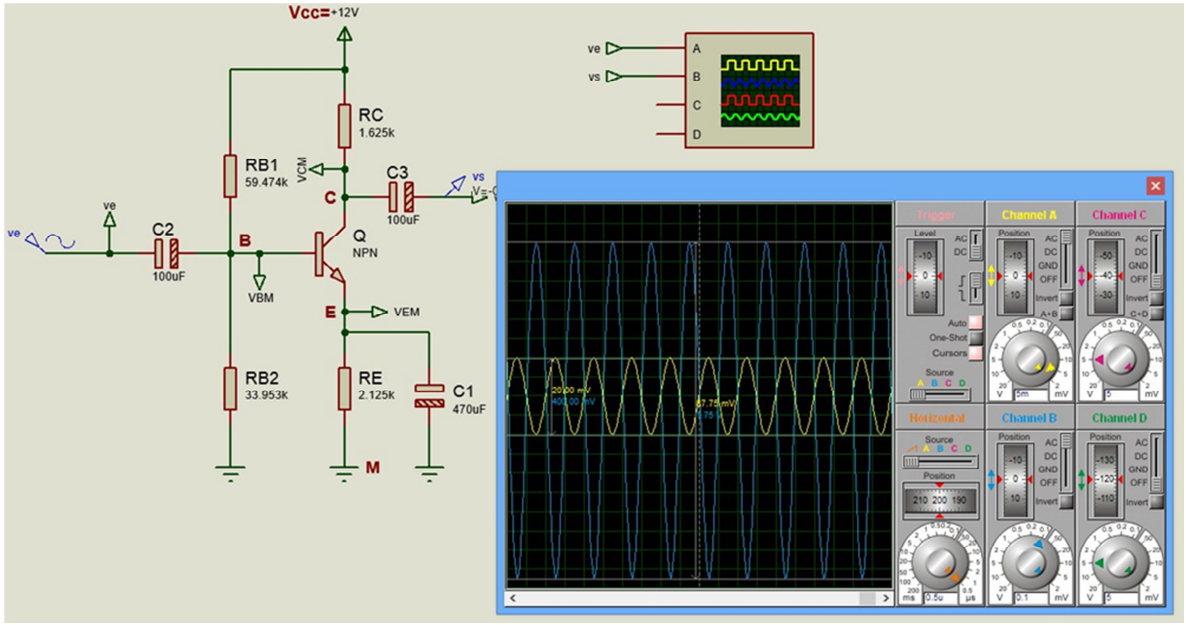

Figure 2: Dynamic results of a common-emitter amplifier with a decoupled emitter using our custom transistor (f = 1 MHz)

4.4.2 Frequency Response Analysis of the Common-Emitter Amplifier

The frequency response simulation of the amplifier in Figure 1 allowed us to plot the curve of voltage gain as a function of frequency (Figure 3).

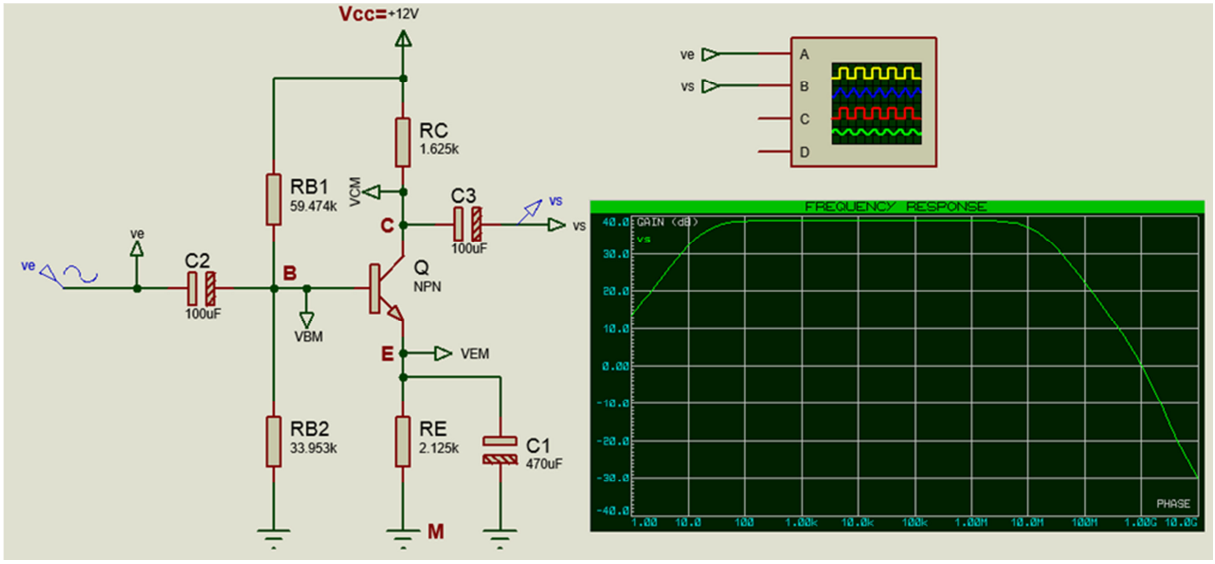

a)

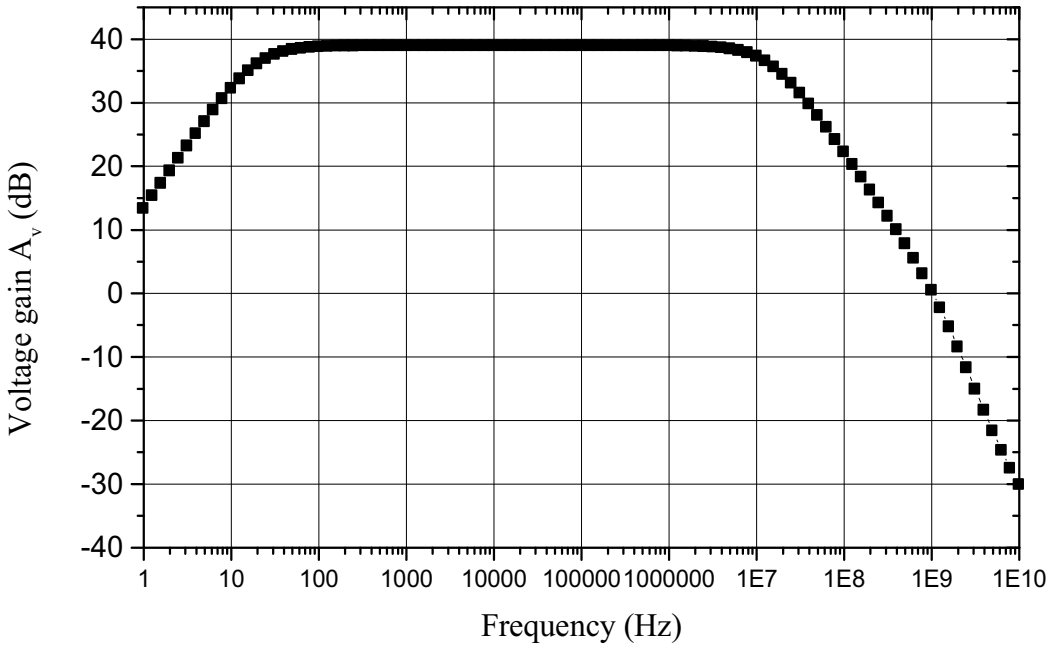

b)

Figure 3: Frequency response of the amplifier with a custom transistor a) Simulated in Proteus b) Processed in ORIGIN 50

We have thus observed that the obtained transition frequency f_T is 1 GHz, which perfectly matches the value initially set during the model creation from the .lib file.

These static and dynamic results confirm that our custom transistor behaves as expected, thereby validating the effectiveness of the implementation method used.

4.4.3 Conclusion

Through this practical section, we successfully validated the implementation of a custom transistor model in Proteus using a .lib file. After creating and integrating the component, we verified its behavior by performing static biasing, which matched the results previously obtained with a standard transistor from the Proteus library.

Furthermore, the frequency response analysis of the common-emitter amplifier confirmed that the transition frequency f_T indeed reached 1 GHz, the value we had specified during the model design.

These results demonstrate that the adopted method allows for the creation of reliable components that accurately reflect the targeted characteristics, paving the way for the development of custom models for specific electronic applications.

4.5 General Conclusion

This chapter has comprehensively presented the design, implementation, and validation of a high-frequency bipolar transistor model in Proteus. Through a theoretical analysis of SPICE parameters (junction capacitances, transit time, current gain, internal resistances), we defined and adjusted a custom model targeting a transition frequency f_T of 1 GHz for a collector current of 1.6 mA. The integration process of the .lib file in Proteus, supported by either creating or reusing a symbol, enabled the generation of a functional component within the simulation environment.

The static results (resting points identical to those obtained with the standard component) and dynamic results (frequency response confirming f_T = 1 GHz) validated the model's accuracy. This approach highlights the importance of a precise balance between electrical parameters and practical constraints to achieve optimal high-frequency performance.

Ultimately, the methodology developed here provides a solid foundation for the creation and evaluation of custom transistor models, paving the way for the design of RF and UHF circuits tailored to specific application needs.

Bibliographic References

[1] A. Sedra & K. Smith, Microelectronic Circuits, 7th ed., Oxford University Press, 2014.

[2] P. E. Gray, P. J. Hurst, S. H. Lewis & R. G. Meyer, Analysis and Design of Analog Integrated Circuits, 5th ed., Wiley, 2009.

[3] Labcenter Electronics, Proteus 8 User Guide, Labcenter Electronics Ltd., 2018.

[4] National Semiconductor, AN-31 Application Note: SPICE Modeling, 2000.

[5] R. J. Baker, CMOS: Circuit Design, Layout, and Simulation, 3rd ed., Wiley-IEEE Press, 2010.

General Conclusion and Perspectives

This final-year project has provided an in-depth exploration of the behavior of analog amplifiers through an approach that integrates solid theoretical foundations, rigorous simulations, and advanced modeling. By focusing on bipolar junction transistor (BJT) amplifiers and operational amplifiers (op-amps), we have highlighted key parameters that govern their frequency behavior, such as static gain, transition frequency (f_T), and internal parasitic effects.

Using the Proteus 8 Professional environment, we validated analytical models derived from the Benahmed method through simulations, demonstrating strong coherence between the theoretical transfer function expressions and the actual dynamic behaviors observed. The precise extraction of bias parameters, coupled with detailed frequency analysis, enabled the design of robust amplifiers well-suited for extended bandwidth requirements.

One of the original contributions of this project is the creation and integration of a hypothetical SPICE model of an ultra-high-frequency transistor (f_T = 1 GHz), expanding simulation possibilities beyond the physical limits of standard components. This approach aligns with a forward-looking vision, aiming at the development of high-performance analog circuits for advanced applications in telecommunications, signal processing, and instrumentation.

Several future directions can be considered based on this work:

Multi-stage optimization: The design of multi-stage amplifiers, incorporating differential configurations or active loads, could achieve higher gains while maintaining bandwidth control.

Integrated design: A relevant perspective would be the transition of these models into microelectronics implementation, particularly through Cadence or LTspice simulations in CMOS technology.

Incorporating non-linearities: Introducing non-linear effects such as harmonic distortion and gain compression in analytical models would allow for a more realistic assessment of performance under extreme dynamic conditions.

System-oriented applications: Integrating the developed circuits into complete systems (active filtering, sensor conditioning, analog modulators) would validate their functional relevance in real-world applications.

Overall, this project has served as a structuring step in mastering techniques for modeling, simulation, and optimization of analog circuits, while opening valuable perspectives for further developments towards more complex and high-performance electronic systems.

الملخص

يركز هذا المشروع على تحليل ونمذجة ومحاكاة دوائر المضخمات التماثلية المعتمدة على الترانزستورات الثنائية القطبية والمضخمات العملياتية. يهدف إلى تقييم أداء هذه الدوائر في المجال الترددي باستخدام أدوات المحاكاة. كما يتضمن إنشاء نموذج افتراضي لمحاكاة التطبيقات التي تعمل في ترددات عالية جدًا. يساهم هذا المشروع في تطوير المهارات في تصميم الدوائر التماثلية والنمذجة والتحليل، ويفتح آفاقًا نحو أنظمة إلكترونية أكثر تقدمًا وتعقيدًا.

الكلمات المفتاحية

المضخمات التناظرية، الترانزستورات ثنائية القطب، المضخمات العملياتية، المحاكاة في المجال الترددي، دالة الانتقال، النمذجة باستخدام، النموذج الافتراضي، تصميم الدوائر، التردد العالي جداً.

Summary

This final-year project focuses on the analysis, modeling, and simulation of analog amplifier circuits based on bipolar junction transistors and operational amplifiers. It uses simulation tools to assess the frequency-domain performance of such circuits. The project also involves the development of a fictitious SPICE model for simulating very high-frequency applications. It strengthens skills in analog circuit design, mathematical modeling, and simulation, while paving the way for more advanced electronic systems.

Keywords

Analog amplifiers, bipolar junction transistors, operational amplifiers, ISIS-Proteus, frequency-domain simulation, transfer function, SPICE modeling, fictitious model, circuit design, very high frequency (VHF)

Résumé

Ce projet de fin d’études porte sur l’analyse, la modélisation et la simulation de circuits amplificateurs analogiques à base de transistors bipolaires et d'amplificateurs opérationnels. Il s’appuie sur des outils de simulation pour évaluer les performances des circuits dans le domaine fréquentiel. Le travail inclut également la création d’un modèle SPICE fictif permettant de simuler des applications à très haute fréquence. Ce projet a permis de renforcer les compétences en conception de circuits analogiques, en modélisation mathématique et en simulation, tout en ouvrant la voie à des systèmes électroniques plus avancés.

Mots clés

Amplificateurs analogiques, transistors bipolaires, amplificateurs opérationnels, ISIS-Proteus, simulation fréquentielle, fonction de transfert, modélisation SPICE, modèle fictif, conception de circuits, très haute fréquence (THF).